Contents lists available at ScienceDirect

Organic Geochemistry

journal homepage: www.elsevier.com/locate/orggeochem

Geochemical characterization of lacustrine and marine oils from off-shore Brazilian sedimentary basins using negative-ion electrospray Fourier transform ion cyclotron resonance mass spectrometry (ESI FTICR-MS)

Ygor dos Santos Rocha [a,b,*], Rosana Cardoso Lopes Pereira [a], João Graciano Mendonça Filho [a,c]

[a] Federal University of Rio de Janeiro (UFRJ), Institute of Geosciences, Av. Athos da Silveira, 274, Prédio do CCMN, Cidade Universitária, 21.949-900 Rio de Janeiro, RJ, Brazil
[b] Division of Geochemistry, PETROBRAS Research and Development Center (CENPES), Av. Horácio Macedo, 950, Cidade Universitária, 21.941-915 Rio de Janeiro, RJ, Brazil
[c] Palynofacies and Organic Facies Laboratory (LAFO)/DEGL/IGEO/CCMN/UFRJ, Av. Athos da Silveira, 274 – Prédio do CCMN, Sala JI-020, Cidade Universitária, 21.941-916 Rio de Janeiro, RJ, Brazil

ARTICLE INFO

ABSTRACT

Lacustrine and marine crude oils from different off-shore Brazilian basins were analyzed using a 7.2 Tesla LTQ FTICR-MS instrument. The samples were analyzed via electrospray ionization in the negative ion mode focusing on the polar compounds, i.e., nitrogen-, sulfur-, and oxygen-containing (NSO) compounds. We also employed a combination of other geochemical methods, such as GC-FID and GC-MS analyses, to characterize and assess the depositional environments of the different oil families. The results indicate that lacustrine oils tend to be enriched in Nx compounds, while marine oils show preference for Ox compounds. The dominant heteroatomic classes in crude oils are N1, followed by O1, O2, and N1O1 with remarkable differences in their distributions between marine and lacustrine, strongly suggesting the control by the kerogen type of the heteroatomic compounds found in these crude oils. Considerable differences in the DBE distribution of the main classes analyzed between the crude oils allowed an efficient geochemical characterization regarding their origin. The use of negative ESI FTICR-MS as a geochemistry tool can provide additional information beyond that obtained with currently employed geochemical methods, resulting in the full comprehension of crude oil composition.

© 2018 Elsevier Ltd. All rights reserved.

1. Introduction

The Brazilian offshore basins along the South Atlantic margins have attracted exploratory interests, mainly after the Pre-Salt discoveries. This sector includes a large number of oil-bearing basins, including Santos, Campos, Espírito Santo, Potiguar, and Sergipe-Alagoas basins, which are the most prolific basins in Brazil. Many relevant studies were carried out on the oil and source-rock samples from these basins for a geochemical assessment of the depositional environments (Mello et al., 1988, 1993, 2012; Schiefelbein et al., 1999, 2000; Katz and Mello, 2000). These authors suggested that oils from these basins were generated under different environmental conditions for source-rock deposition, ranging from lacustrine freshwater to marine systems.

Gas chromatography coupled to mass spectrometry (GC-MS) has been one of the most important techniques used to assess biomarkers for geochemical characterization. Comprehensive two-dimensional gas chromatography instruments (GC × GC), since they became commercially available, have improved analyses and been used for advanced biomarker evaluation (Casilli et al., 2014). Eleven Brazilian crude oils from different source rocks and depositional environments have been analyzed by GC × GC using high-resolution molecular organic geochemistry (Laakia et al., 2017). Even unusual biomarkers can be revealed by this technique, the majority of these previous studies focused only on hydrocarbons.

The advent of Fourier transform ion cyclotron resonance mass spectrometry (FTICR-MS) has changed the way of characterizing crude oil samples and allowed a scrutiny of their polar composition at the molecular level. The ultra-high resolution and accuracy of FTICR-MS are ideal for the analysis of complex mixtures, allowing the assignment of detected masses to chemical formulas (Marshall et al., 2007). When coupled with the electrospray ionization (ESI)

technique, which produces molecular ions, the composition of selective polar species can be characterized in detail (Qian et al., 2001). In addition, application of polar compound study to the geochemical characterization is promising because of its potential to resolve cases where traditional biomarkers are not sufficiently conclusive (e.g., the case where samples are contaminated by drilling fluid which has more than 90% of hydrocarbons in its composition).

This field, known as "petroleomics" (Rodgers et al., 2005), is now applied to geochemistry studies in order to determine the distribution of non-hydrocarbon compounds in petroleum from different sources and to identify changes in their distribution during biodegradation, expulsion and migration fractionation, thermal evolution or water washing (e.g., Kim et al., 2005; Hughey et al., 2007; Tong et al., 2013; Vaz et al., 2013; Oldenburg et al., 2014, 2017; Liu et al., 2015; Mahlstedt et al., 2016; Wan et al., 2017; Rocha et al., 2018). Despite these advances, there is still a lack of information about the relationship between different environmental conditions for source-rock deposition and the composition of heteroatomic compounds in Brazilian crude oils.

Recently, Wan et al. (2017) have characterized the polar compounds, by negative ESI FTICR-MS, in terrestrial oils and rock samples from the Nanpu Sag (China) and concluded that the source input directly controls the distribution of heteroatomic compounds. In this study, a combination of bulk geochemical methods and negative-ion ESI FTICR-MS were employed to study several oil samples and to characterize and assess the depositional environments of different oil families recovered from four different basins from Brazilian marginal coast.

2. Geological background

The Brazilian continental margin basins (Supplementary Fig. 1) are directly related to the break-up of the Gondwana supercontinent (Contreras et al., 2010). According to these authors, and references therein, the development of these basins includes five major stages of basin evolution: (i) pre-rift; (ii) syn-rift; (iii) syn-rift sag; (iv) post-rift; (v) drift. Several basins have been described, including (from north to south) Foz do Amazonas, Barreirinhas, Ceará, Potiguar, Sergipe–Alagoas, Recôncavo, Espírito Santo, Campos, Santos, and Pelotas (Schiefelbein et al., 2000). They were formed during an Early Cretaceous rifting phase, responsible for the sedimentation of a thick succession containing continental, fluvial and lacustrine siliciclastic and carbonate sediments (Mello et al., 1988). Frequent marine ingression into these restricted basin systems, formed by ongoing thermal subsidence, caused a change in the sedimentary deposition in the Late Aptian to a purely evaporitic deposition from a hyper saline system (Strozyk et al., 2017). As a result of sea floor spreading and the subsidence of the Brazilian continental margin, the proto-South Atlantic Ocean kept a practically uniform paleogeographic during the Albian, responsible for the carbonate sedimentation that was accumulated in an epicontinental sea (Mello et al., 1988). The late Cretaceous to Holocene marine shelf-slope succession, characterized by carbonate and mainly siliciclastic sediments, represents the open marine stage in the Brazilian marginal basins.

3. Samples and methods

3.1. Samples

Sixty-nine oil samples (Table 1) from four different off-shore Brazilian basins were selected for analyses. Two basins produce oils from mostly lacustrine origin while the other two are known for their production of marine oils. The selection of oils was designed to avoid any kind of secondary alteration such as biodegradation, water-washing, or secondary-cracking. Moreover, all these samples were generated in the peak oil window (Supplementary Fig. 2).

Table 1
Distribution of the selected oils from Brazilian off-shore basins.

| Basin	Field	Sample number	Source rock environmental
Basin A	Field A.1	#01	Lacustrine
		#02	
	Field A.2	#03	
	Field A.3	#04	
	Field A.4	#05	
		#06	
		#07	
		#08	
		#09	
		#10	
Basin B	Field B.1	#11	Marine
		#12	
		#13	
		#14	
	Field B.2	#15	
		#16	
	Field B.3	#17	
		#18	
		#19	
		#20	
		#21	
		#22	
		#23	
		#24	
	Field B.4	#25	
		#26	
	Field B.5	#27	
		#28	
Basin C	Field C.1	#29	Marine
		#30	
		#31	
	Field C.2	#32	
		#33	
		#34	
		#35	
	Field C.3	#36	
		#37	
	Field C.4	#38	
		#39	
	Field C.5	#40	
		#41	
Basin D	Field D.1	#42	Lacustrine
		#43	
	Field D.2	#44	
		#45	
		#46	
		#47	
	Field D.3	#48	
		#49	
	Field D.4	#50	
		#51	
		#52	
		#53	
	Field D.5	#54	
	Field D.6	#55	
		#56	
		#57	
		#58	
		#59	
		#60	
		#61	
		#62	
		#63	
	Field D.7	#64	
	Field D.8	#65	
		#66	
		#67	
		#68	
	Field D.9	#69	

3.2. GC-FID and GC-MS analysis

Approximately 50 mg of each crude oil sample was diluted in 1 mL of dichloromethane and analyzed by GC. The GC analyses were performed with an Agilent 7890B gas chromatograph equipped with a split/splitless injector and a flame ionization detector (FID). A fused silica DB-5 phenyl/methyl polysiloxane

capillary column (30 m × 0.25 mm × 0.25 µm; Agilent Technologies) was used, and the oven temperature was programmed from 40 °C to 320 °C at a heating rate of 2.5 °C/min. Helium was used as a carrier gas at a constant flow of 1.3 mL/min.

Approximately 60 mg of each crude oil sample was weighed, dissolved in n-hexane, and spiked with an appropriated quantity of internal standard β-cholane. After homogenization, the mixture
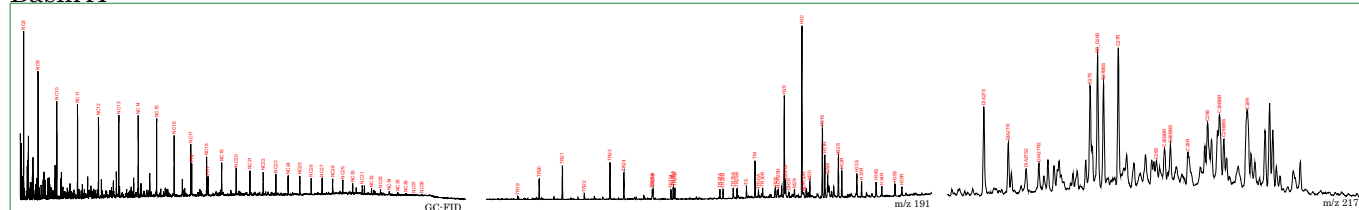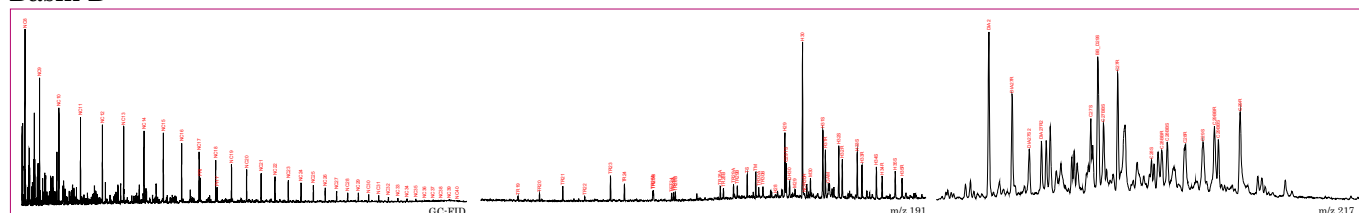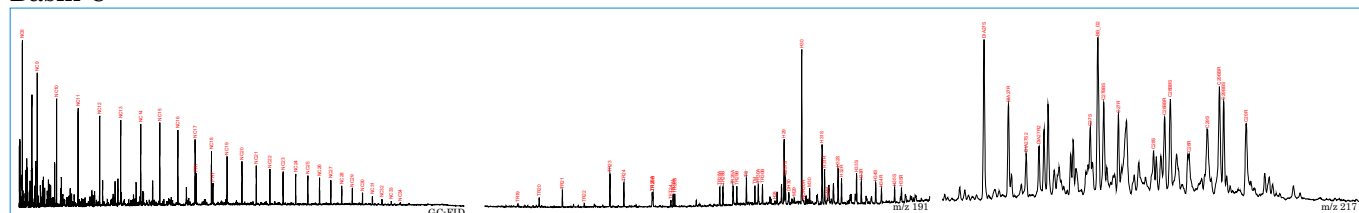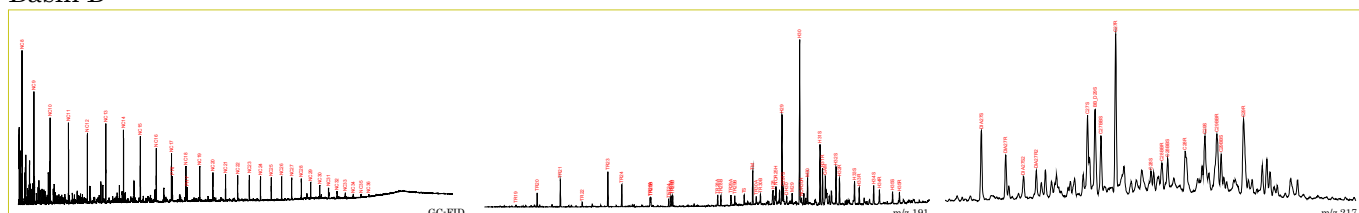

Fig. 1. Whole oil gas chromatograms (left), terpane distributions – m/z 191 (center) and steranes distributions – m/z 217 (right) of representative oils from basins A, B, C and D. Oils from basins A and D have typical features of lacustrine oils whereas oils from basins B and C are related to a marine origin.

Fig. 2. Cross-plots of typical source parameters using saturated biomarkers: Hopanes/Steranes vs. TPP/(TPP + DIAS) and %C$_{27}$ sterane vs. %C$_{29}$ sterane. It is possible to indicate a lacustrine origin of the Basin A and D oils, and a marine origin of the Basin B and C oils.

was injected into a Margot Köhnen-Willsch (MKW) semi-automated medium pressure liquid chromatography (MPLC) to obtain saturated hydrocarbon fractions.

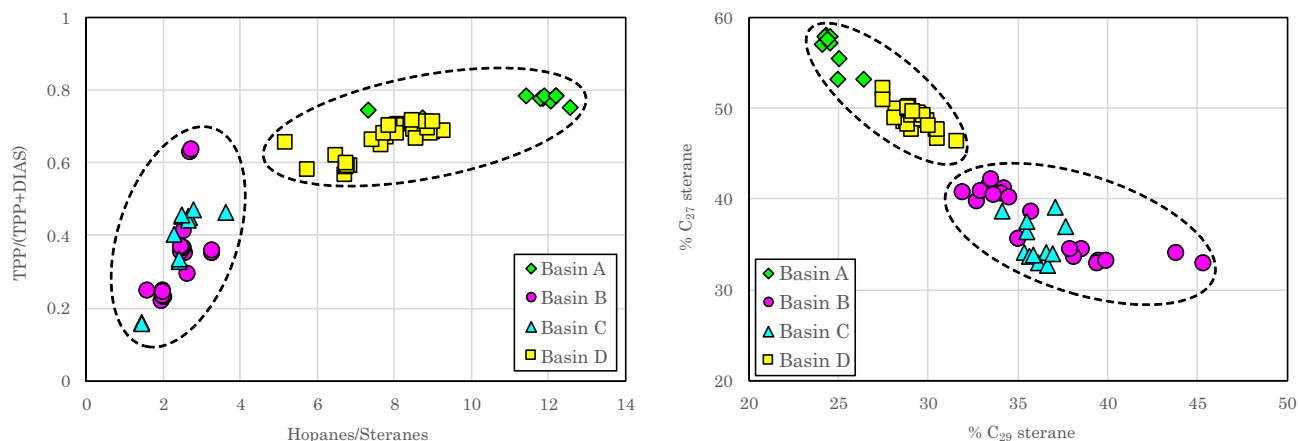Analysis of the saturated fractions by gas chromatography coupled to mass spectrometry (GC/MS) was carried out on an Agilent 7890B GC equipped with a split/splitless injector and interfaced to an Agilent 5977A quadrupole mass selective detector. The separation of saturated hydrocarbon fractions was achieved by injecting the mixture into a DB-5 fused silica capillary column (60 m × 0.25 mm × 0.25 μm; Agilent Technologies). The GC oven was temperature-programmed from 55 °C as an initial temperature (held for 2 min) to 150 °C at 20 °C/min, followed by a second gradient of 1.5 °C/min to a final temperature of 320 °C (held for 20 min). Aliquots of 1 μL of the saturated hydrocarbon fraction were injected into the GC system in splitless mode. High-purity helium (99.999%) was used as the carrier gas under constant flow mode at a rate of 1.6 mL/min. The mass spectrometer was operated in electron impact mode at 70 eV, at a source temperature of 230 °C and a quadrupole temperature of 150 °C. The samples were analyzed in

selected ion monitoring (SIM) mode. The concentrations of selected biomarkers relative to the whole oil were determined by comparing the peak areas in selected ions chromatogram to that of the internal standard β-cholane. Response factors for the components of interest relative to the internal standard were assumed to be 1.0.

3.3. ESI FTICR-MS analysis

Mass analyses were performed in negative ion ESI mode using a 7.2 Tesla LTQ FT Ultra mass spectrometer (Thermo Scientific, Bremen, Germany). Crude oil samples (1 mg) were dissolved in 1 mL of toluene and then diluted with 1 mL of methanol containing 0.1% of ammonium hydroxide. All solvents used for sample preparation were HPLC grade and purchased from Sigma-Aldrich. Samples were loaded into a 500 μL Hamilton syringe and analyzed. The general ESI conditions were as follows: spray voltage of 3.5 kV, tube lens voltage of −140 V, and a flow rate of 5 μL/min. Mass spectra were the result of over 100 microscans processed via the Xcalibur 2.0 software (ThermoScientific, Bremen, Germany).
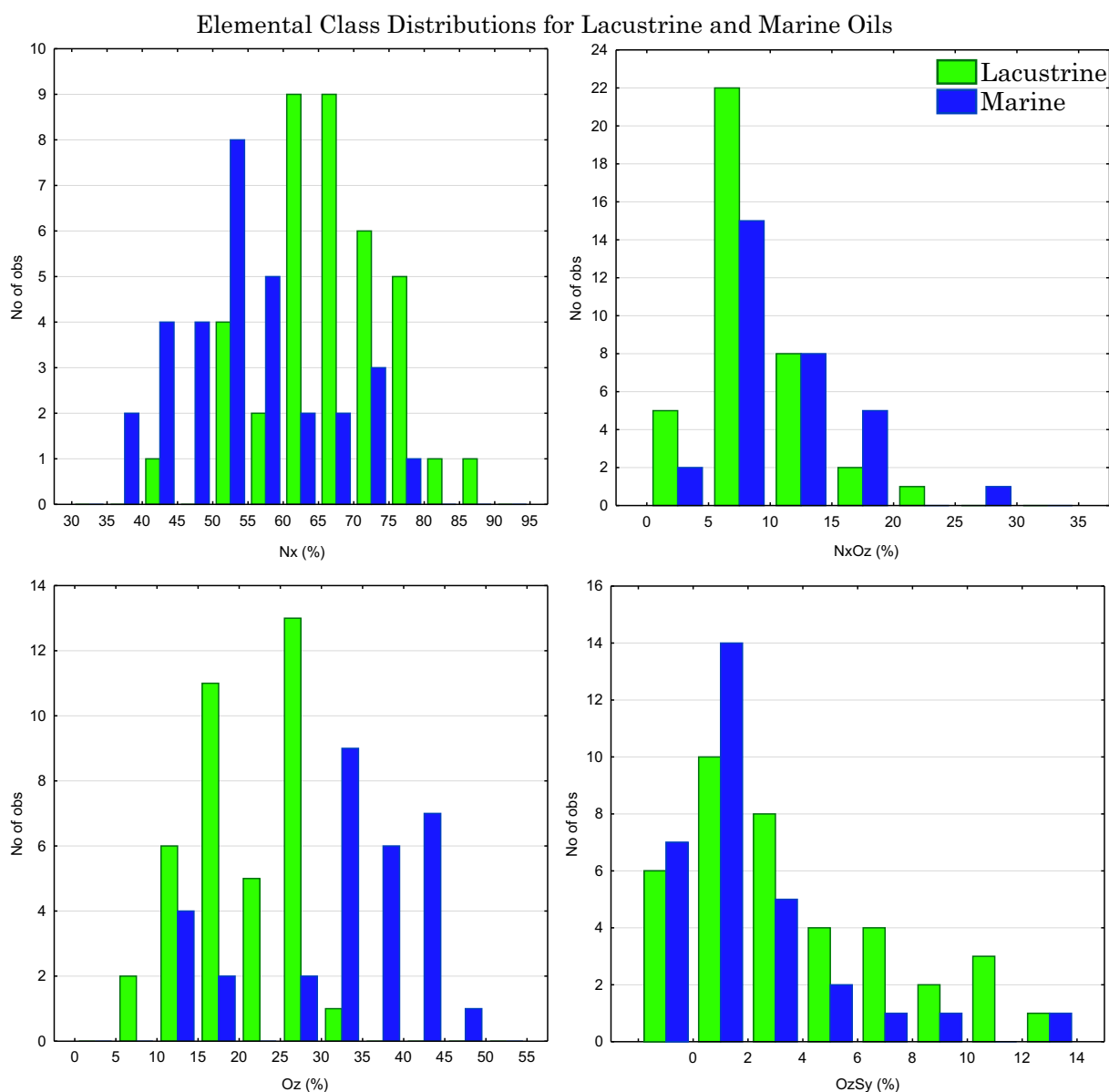

Fig. 3. Histograms displaying the elemental class distribution of the negative ESI FTICR-MS results from the 69 samples analyzed. The samples were splitted in two domains: marine and lacustrine oil samples.

3.4. Data processing

Data processing was performed using the Petro MS software developed by Petrobras and UNICAMP (State University of Campinas) for formula attribution and recalibration of known homologous series from the measured m/z values of polar crude oil compounds. Elemental formulas were calculated and assigned on the basis of the m/z values within an error range of 1 ppm. For each spectrum, automated analysis was used to assign formulas to peaks with a signal-to-noise ratio > 3. The selected elements were ^{12}C, ^{13}C, ^{1}H, ^{16}O, ^{14}N, ^{32}S, and ^{34}S. Data analysis and visualization were performed using the Ragnarök software (Aphorist Inc.), a data processing software tool for visualization and interpretation of multi-dimensional and multi-sample FTICR-MS data. Apart from the determination of molecular masses and double bond equivalents [DBE comes from $(C_cH_hN_nS_sO_o) = c - h/2 + n/2 + 1$] of detectable individual species in whole oils or bitumen fractions, the Ragnarök software also grouped abundances of whole heteroatom classes (a heteroatom class is a group of compounds with a uniform heteroatom population), DBE distributions within a heteroatom class, carbon number distributions for all the attributed compounds and a variety of plots, including ternary diagrams.

3.5. Statistical data treatment

After ESI FTICR-MS analysis, hierarchical clustering (HCA), principal component analysis (PCA), and histograms were performed on the experimental data. Detailed information about these analyses can be found in the literature (Miller and Miller, 2010). Exploratory data analysis was applied to the data matrix consisting of the sixty-nine samples (as rows) and this group of variables (as columns). Statistica version 12 (StatSoft, www.statsoft.com, USA) was used for statistical analyses.

4. Results and discussion

4.1. Geochemical characterization: biomarker analysis

All sixty-nine samples were classified based on the characteristics of oils from Brazilian off-shore basins published by Mello et al. (1988, 1993, 1995, 1995, 2012). The distribution of saturated biomarkers from these four basins (Fig. 1) reveals differences related to the paleoenvironmental conditions of their source rocks. Using conventional geochemical parameters (Peters et al., 2005; Dembicki, 2016) such as hopane/sterane ratio, tetracyclic polyprenoids (TPP) ratio (TPP/TPP + diasteranes, measured at m/z 259), and steranes distribution, it is possible to verify that oils from basins A and D have typical features of lacustrine oils and samples from basins B and C have typical features of source rocks deposited in marine environments (Fig. 2 and Supplementary Table 1).

4.2. General chemical composition

Based on the previously mentioned geochemical characterization, all samples were split into two groups according to their depositional environments (marine or lacustrine samples – Table 1).

Table 2
Elemental and compound classes distributions for lacustrine oils samples.

Sample number	Elemental classes (%)				Compound classes distribuition (%)																
	N_x	N_xO_z	O_z	O_2S_y	N	NO	NO_2	NO_3	O	O_2	O_3	O_4	O_5	OS	O_2S	O_3S	O_4S	O_6S	O_6S_2	OS_3	O_2S_3
#01	85.6	4.5	8.9	1.0	85.6	3.7	0.8	–	6.4	1.9	0.6	–	–	–	–	–	–	–	1.0	–	–
#02	81.4	8.4	8.3	1.9	81.4	6.7	1.7	–	6.9	1.4	–	–	–	–	–	–	0.6	–	–	0.7	0.6
#03	71.3	6.8	18.2	3.7	71.3	5.2	1.6	–	10.6	5.9	1.7	–	–	–	–	–	2.5	–	–	0.6	0.6
#04	56.4	11.4	19.8	12.4	56.4	7.1	3.2	1.1	10.9	7.4	0.6	0.5	0.4	–	–	3.8	7.9	–	0.7	–	–
#05	67.2	7.8	14.3	10.7	67.2	6.8	1.0	–	9.9	4.4	–	–	–	–	–	2.0	8.7	–	–	–	–
#06	69.0	7.8	14.9	8.3	69.0	6.8	1.0	–	10.3	4.6	–	–	–	–	–	–	8.3	–	–	–	–
#07	64.4	10.1	14.1	11.4	64.4	8.5	1.6	–	8.5	5.6	–	–	–	–	–	2.3	9.1	–	–	–	–
#08	69.4	7.7	14.2	8.7	69.4	6.8	0.9	–	9.8	4.4	–	–	–	–	–	2.0	6.7	–	–	–	–
#09	69.2	8.2	14.7	7.9	69.2	7.0	1.2	–	10.2	4.5	–	–	–	–	–	–	7.9	–	–	–	–
#10	67.3	8.8	13.7	10.2	67.3	7.4	1.4	–	9.8	3.9	–	–	–	–	–	–	10.2	–	–	–	–
#42	50.8	15.6	32.2	1.4	50.8	9.9	4.3	1.4	13.1	19.1	–	–	–	–	–	–	–	0.7	–	0.7	–
#43	57.4	15.0	27.6	–	57.4	10.8	4.2	–	11.4	16.2	–	–	–	–	–	–	–	–	–	–	–
#44	43.6	21.7	28.9	5.8	43.6	12.6	7.5	1.6	10.3	18.0	0.6	–	–	–	–	2.9	2.9	–	–	–	–
#45	54.8	14.1	28.3	2.8	54.8	8.7	5.4	–	12.4	15.9	–	–	–	–	–	1.6	1.2	–	–	–	–
#46	64.2	6.4	22.0	7.4	64.2	4.6	1.8	–	11.3	10.7	–	–	–	–	–	2.2	–	3.2	–	2.0	–
#47	63.3	9.0	25.8	1.9	63.3	5.4	3.6	–	12.2	13.6	–	–	–	–	–	1.9	–	–	–	–	–
#48	70.8	10.0	15.6	3.6	70.8	6.6	2.8	0.6	10.8	4.8	–	–	–	–	–	1.3	1.1	–	–	0.9	0.3
#49	73.5	4.3	22.2	–	73.5	3.7	0.6	–	16.3	5.9	–	–	–	–	–	–	–	–	–	–	–
#50	68.1	11.3	20.0	0.6	68.1	7.8	3.5	–	12.4	7.6	–	–	–	–	–	–	0.6	–	–	–	–
#51	77.4	5.4	15.9	1.3	77.4	4.6	0.8	–	8.6	4.9	2.4	–	–	0.8	0.5	–	–	–	–	–	–
#52	78.3	3.8	17.9	–	78.3	2.9	–	0.9	9.6	7.1	1.2	–	–	–	–	–	–	–	–	–	–
#53	77.4	5.0	15.5	2.1	77.4	3.7	1.3	–	11.1	4.4	–	–	–	–	–	–	–	–	–	2.1	–
#54	51.3	16.1	28.7	3.9	51.3	10.7	4.6	0.8	15.6	13.1	–	–	–	–	–	1.9	1.4	–	0.6	–	–
#55	60.6	11.5	22.5	5.4	60.6	7.4	2.7	1.4	11.9	7.4	1.3	1.6	0.3	–	–	2.4	1.4	–	1.6	–	–
#56	70.9	6.8	22.3	0.0	70.9	4.5	2.3	–	12.9	9.4	–	–	–	–	–	–	–	–	–	–	–
#57	73.3	6.4	17.5	2.8	73.3	4.9	1.5	–	10.9	4.1	1.9	0.6	–	–	–	–	1.6	–	1.2	–	–
#58	76.4	6.0	16.0	1.6	76.4	4.8	1.2	–	12.6	3.4	–	–	–	–	–	–	1.1	–	–	0.5	–
#59	72.8	8.5	17.3	1.4	72.8	6.5	2.0	–	12.8	4.5	–	–	–	–	–	–	1.4	–	–	–	–
#60	76.9	5.3	16.5	1.3	76.9	4.4	0.9	–	12.4	4.1	–	–	–	–	–	–	–	–	–	1.3	–
#61	61.2	10.9	25.3	2.6	61.2	7.3	3.6	–	13.1	12.2	–	–	–	–	–	2.6	–	–	–	–	–
#62	61.7	8.6	25.5	4.2	61.7	5.9	2.7	–	12.2	13.3	–	–	–	–	–	1.4	1.6	–	–	1.2	–
#63	60.1	5.4	28.0	6.5	60.1	3.3	1.5	0.6	11.5	15.6	0.9	–	–	–	–	3.8	1.3	–	1.4	–	–
#64	65.8	8.6	25.6	–	65.8	5.6	3.0	–	13.1	12.5	–	–	–	–	–	–	–	–	–	–	–
#65	51.8	13.4	30.0	4.8	51.8	8.0	4.6	0.8	11.9	16.6	1.5	–	–	–	–	2.7	1.3	–	0.8	–	–
#66	62.8	4.0	26.8	6.4	62.8	2.6	1.4	–	10.9	15.9	–	–	–	–	–	–	–	–	–	4.8	1.6
#67	65.1	8.7	25.4	0.8	65.1	5.0	3.1	0.6	12.3	11.7	1.4	–	–	–	–	–	–	–	0.8	–	–
#68	66.8	8.0	22.0	3.2	66.8	5.3	2.7	–	9.1	12.9	–	–	–	–	–	–	–	–	–	3.2	–
#69	64.8	7.4	27.8	–	64.8	4.2	3.2	–	11.8	16.0	–	–	–	–	–	–	–	–	–	–	–

The main differences in the distribution of polar compounds between the two groups were evaluated.

4.2.1. Elemental class distributions

The elemental class distributions of lacustrine oils are compared to those of marine oils using histograms as shown in Fig. 3 (data in Tables 2 and 3). The first significant difference between the two groups is related to the Nx and Oz classes, which dominate the acidic compound fraction of all samples. Lacustrine oils tend to be enriched in Nx compounds (lacustrine oils: 43.60–85.60% – average: 66.40%; marine oils: 37.80–75.70% – average: 54.58%), while marine oils can be distinguished by their preference for Ox compounds (lacustrine oils: 8.30–32.20% – average: 20.79%; marine oils: 11.30–47% – average: 32.20%). Sulfur-containing classes (OzSy) are present in a lower amount in both systems, and NxOz compounds show a similar distribution in oil samples regardless of the depositional environments of the source rocks. The oil samples were tentatively separated based on the relative amounts of the three major elemental classes: Nx, Oz, and NxOz as shown in the ternary diagram (Fig. 4). Although the two domains cannot be entirely separated, the results suggest that polar compound distribution could be related to their original content of organic matter that was deposited under different environmental conditions.

4.2.2. Compound class distributions

Compound class distributions of lacustrine and marine oils are displayed in Tables 2 and 3, respectively. The heteroatomic classes N1, N1O1, N1O2, N1O3, O1, O2, O3, O4, O5, O1S1, O2S1, O3S1, O4S1, O6S1, O6S2, O1S3, and O2S3 were assigned for crude oils. The dominant heteroatom class in crude oils based on the relative abundance values is N1 (lacustrine oils: 43.60–85.60% – average: 66.40%; marine oils: 37.80–75.70% – average: 54.58%), followed by O1 (lacustrine oils: 6.40–16.30% – average: 11.26%; marine oils:
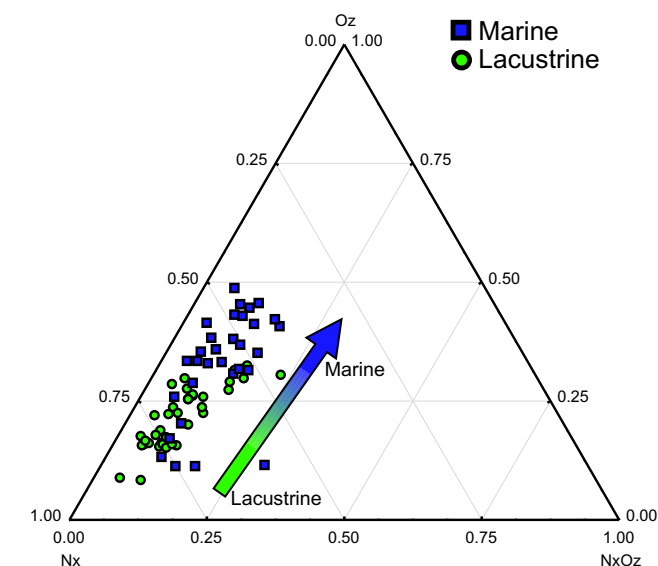
Fig. 4. Ternary diagram for the most abundant Elemental Classes assigned on the negative ESI FTICR-MS results: Nx, Oz, and NxOz.

5–30.90% – average: 19.98%), O_2 (lacustrine oils: 1.40–19.10% – average: 9.08%; marine oils: 3–32.10% – average: 11.28%) and N1O1 (lacustrine oils: 2.60–12.60% – average: 6.26%; marine oils: 3.90–22.30% – average: 8.05%). These findings are very similar to previous studies of crude oils using negative-ion ESI FTICR-MS (Hughey et al., 2002; Cui et al., 2014; Mahlstedt et al., 2016; Wan et al., 2017), indicating a predominance of N1 and O1 species in crude oils.

Table 3
Elemental and compound classes distributions for marine oils samples.

Sample number	Elemental classes (%)				Compound classes distribuition (%)																	
	N_x	N_xO_z	O_z	O_zS_y	N	NO	NO_2	NO_3	O	O_2	O_3	O_4	O_5	OS	O_2S	O_3S	O_4S	O_6S	O_6S_2	OS_3	O_2S_3
#11	53.0	3.9	40.4	2.7	53.0	3.9	–	–	25.1	15.3	–	–	–	–	0.5	–	2.2	–	–	–	–
#12	55.2	5.8	33.5	5.5	55.2	4.6	1.2	–	20.9	12.6	–	–	–	1.5	0.7	–	3.3	–	–	–	–
#13	39.2	9.0	39.2	12.6	39.2	6.7	2.3	–	18.0	20.3	0.9	–	–	2.0	1.3	7.4	1.9	–	–	–	–
#14	37.8	16.0	37.2	9.0	37.8	10.8	4.2	1.0	17.8	17.9	1.5	–	–	1.1	1.6	2.8	3.5	–	–	–	–
#15	43.6	7.6	42.8	6.0	43.6	5.3	2.3	–	14.8	28.0	–	–	–	1.2	1.7	0.9	1.4	–	–	0.8	–
#16	43.8	5.3	47.0	3.9	43.8	3.9	1.4	–	14.9	32.1	–	–	–	1.4	2.5	–	–	–	–	–	–
#17	54.9	14.1	31.0	0.0	54.9	9.5	4.1	0.5	19.7	10.5	0.8	–	–	–	–	–	–	–	–	–	–
#18	51.6	16.6	31.4	0.4	51.6	8.7	6.7	1.2	19.1	11.1	1.2	–	–	–	–	–	0.4	–	–	–	–
#19	45.1	12.7	40.7	1.5	45.1	8.6	3.3	0.8	23.7	12.4	1.8	1.9	0.9	–	–	–	1.5	–	–	–	–
#20	41.0	15.9	41.7	1.4	41.0	9.9	4.7	1.3	26.7	13.9	1.1	–	–	–	–	–	1.4	–	–	–	–
#21	41.4	11.2	44.2	3.2	41.4	7.1	3.4	0.7	26.8	12.0	4.6	0.8	–	1.7	0.6	–	0.9	–	–	–	–
#22	61.9	4.6	33.5	–	61.9	3.9	0.7	–	26.9	4.5	2.0	1.1	–	–	–	–	–	–	–	–	–
#23	62.4	7.8	28.5	1.3	62.4	6.2	1.6	–	17.9	9.5	1.1	–	–	–	–	–	1.0	–	0.3	–	–
#24	67.6	6.0	25.9	0.5	67.6	5.4	0.6	–	17.7	8.2	–	–	–	–	–	–	–	–	–	0.5	–
#25	47.3	8.1	42.2	2.4	47.3	6.4	1.7	–	27.6	13.9	0.7	–	–	1.0	–	–	1.4	–	–	–	–
#26	54.5	6.5	38.0	1.0	54.5	5.8	0.7	–	26.9	11.1	–	–	–	0.5	–	–	0.5	–	–	–	–
#27	56.4	8.3	32.1	3.2	56.4	6.7	1.6	–	24.5	6.8	0.8	–	–	–	–	–	3.2	–	–	–	–
#28	51.4	10.1	30.7	7.8	51.4	8.5	1.6	–	22.8	7.9	–	–	–	–	–	–	7.8	–	–	–	–
#29	55.5	8.4	36.1	–	55.5	6.9	1.5	–	25.6	10.5	–	–	–	–	–	–	–	–	–	–	–
#30	47.5	16.2	34.6	1.7	47.5	11.1	4.3	0.8	20.8	11.5	1.8	0.5	–	–	–	–	0.6	–	–	1.1	–
#31	60.0	6.4	33.6	–	60.0	5.5	0.9	–	26.2	7.4	–	–	–	–	–	–	–	–	–	–	–
#32	58.0	29.1	11.5	1.4	58.0	22.3	5.0	1.8	5.0	5.8	0.7	–	–	–	–	–	–	–	–	1.0	0.4
#33	70.7	16.8	11.4	1.1	70.7	14.1	2.7	–	7.8	3.6	–	–	–	–	–	–	–	1.1	–	–	–
#34	73.5	13.2	11.3	2.0	73.5	11.3	1.9	–	7.9	3.4	–	–	–	–	–	–	–	0.8	–	1.2	–
#35	75.7	9.9	13.2	1.2	75.7	8.8	1.1	–	7.8	3.9	0.7	0.8	–	–	–	–	–	–	1.2	–	–
#36	51.2	10.7	38.1	–	51.2	8.2	2.5	–	22.0	12.1	2.7	1.3	–	–	–	–	–	–	–	–	–
#37	50.6	12.5	36.9	–	50.6	9.3	3.2	–	23.9	12.4	0.6	–	–	–	–	–	–	–	–	–	–
#38	46.8	9.9	42.8	0.5	46.8	7.0	2.9	–	30.9	11.9	–	–	–	–	–	–	0.5	–	–	–	–
#39	53.3	14.9	31.8	–	53.3	10.1	4.4	0.4	19.4	12.4	–	–	–	–	–	–	–	–	–	–	–
#40	72.6	9.4	17.0	1.0	72.6	6.6	2.8	–	14.0	3.0	–	–	–	–	–	–	–	–	–	1.0	–
#41	68.4	9.9	20.0	1.7	68.4	6.4	3.5	–	16.2	3.8	–	–	–	–	–	–	1.7	–	–	–	–

The distribution of these major classes is shown in Fig. 5. It is possible to verify that N1 class is more abundant in lacustrine oils when compared to marine oils, with the latter remarkably enriched in O1 class compounds. The distribution of the N1O1 and O2 classes is very similar between the two groups, only with a slight increase of these compounds in the marine oils, corroborating the results discussed in the Elemental Class Distribution section.

These results are also in agreement with those obtained by Wan et al. (2017), i.e., a predominance of the N1 species but a relatively low content of O$_x$ species in oils derived from source rocks containing Type I kerogen when compared with oils from source rocks containing the Type II and Type III kerogens. The authors also reported a good correlation between oil results and their corresponding source rocks, confirming that organic input has a controlling effect on the heteroatom species in source rocks and oils. Cui et al. (2014) described the polar compounds from lacustrine and marine oil samples using ESI FTICR-MS, and the authors found an enrichment of oxygen-containing compounds in marine oils, consistent with our results.

The widely accepted classification of source rock (Vandenbroucke and Largeau, 2007) divides kerogen into three main types based on elemental analysis. Type I Kerogen (generally associated with lacustrine environment) is highly aliphatic, with an H/C atomic ratio frequently > 1.5. Oxygen content, as well as the content of polyaromatic nuclei and heteroatomic groups is often low (Tissot and Welte, 1984). Organic matter from type II kerogen (associated with marine sediments) contains more polyaromatic nuclei, higher O/C atomic ratio, and abundant carboxylic acid and ester groups (Tissot and Welte, 1984). Vandenbroucke and Largeau (2007) summarized that kerogen composition depends on biological precursors, chemical and biochemical alteration processes, leading to a clear-cut difference between marine and terrestrial kerogens. Thus, characteristics of each kerogen were
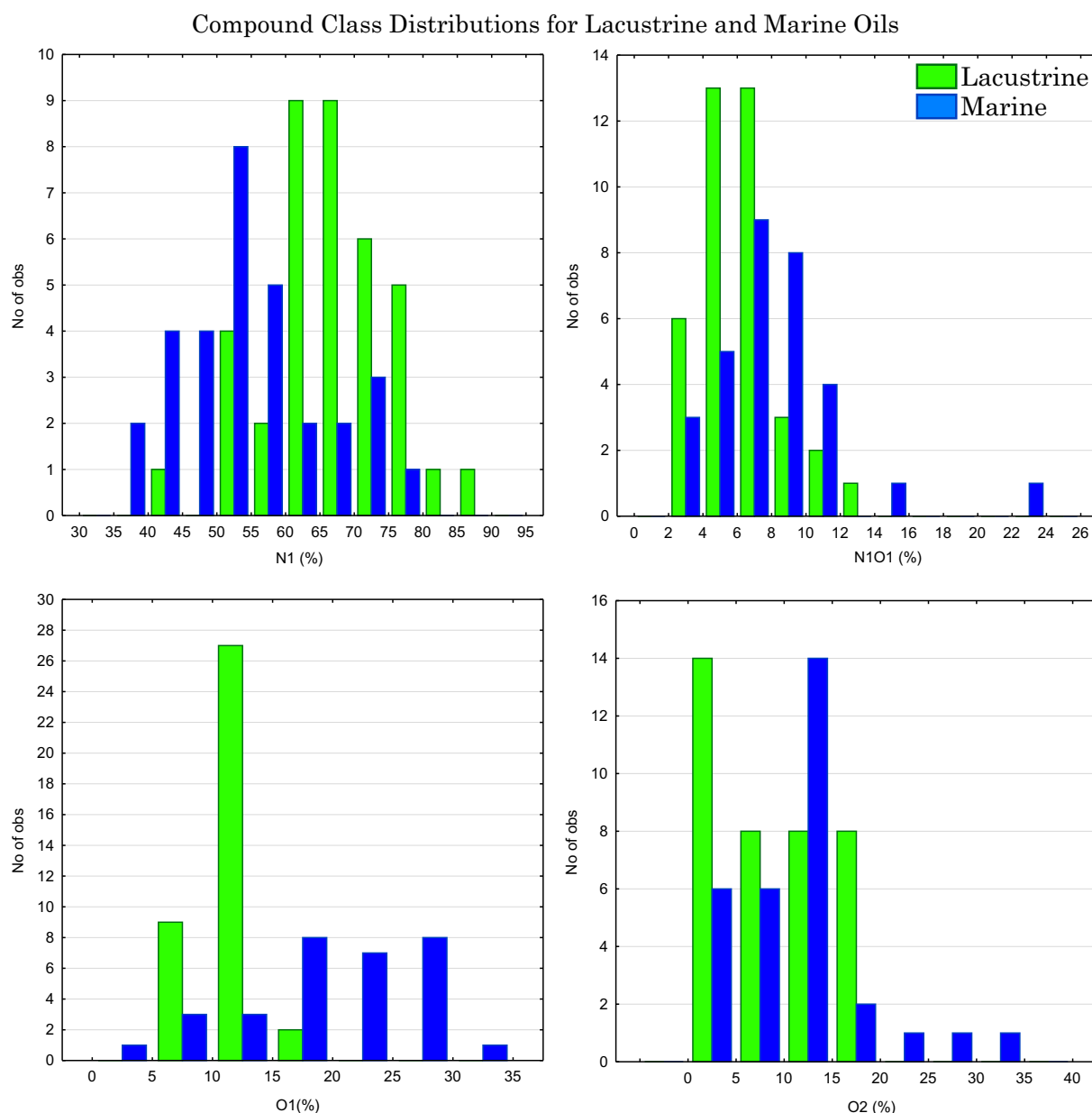
Fig. 5. Histograms displaying the four major compound class distribution on the negative ESI FTICR-MS results from the 69 samples analyzed. The samples were split into two domains: marine and lacustrine oil samples.

considered as the main controlling factor on the distribution of polar compounds in source rock extracts and crude oils.

Considering only the class distributions, HCA analysis was performed using data listed in Tables 2 and 3 in order to evaluate the efficiency of genetic classification of the oils. The application of most of the methods resulted in a division of the 69 samples into two main clusters, based on the sedimentation environment of the organic matter and labeled as Lacustrine and Marine domains (Fig. 6). The best results were obtained using a combination of "1-Pearson r" distance with Ward's method (a method of cluster analysis based on minimalization of the variance in the clusters).

The "1-Pearson r" distance is defined according to a formula that for similar samples the correlation coefficient is close to one and the distance between samples is close to zero (Krawczyk et al., 2005). The exceptions were samples #23–24, #32–35, and #41 (samples of marine origin that were grouped together with lacustrine oils), as well as # 54 (sample of lacustrine origin that was grouped together with marine oils), due to compound class distributions anomaly such as high nitrogen content for the marine oil samples and high content of O1 class for the lacustrine sample. Therefore, the rapid statistical analysis was able to correctly distinguish and separate 88% of crude oil samples into two main groups,
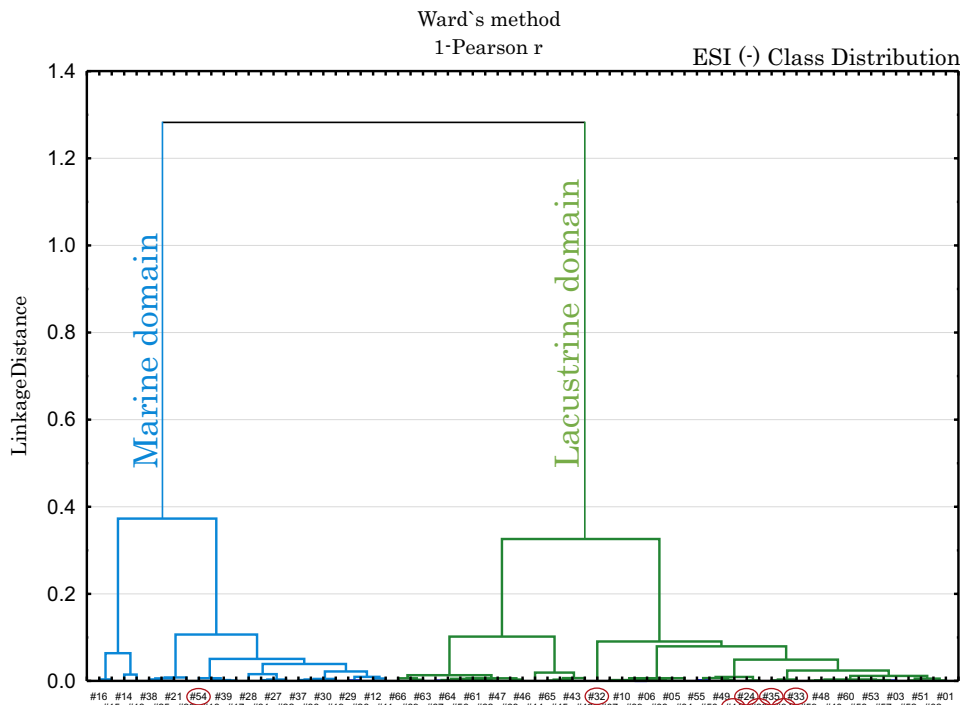
Fig. 6. HCA performed on all compound class distribution assigned in the negative ESI FTICR-MS results from the 69 samples analyzed.
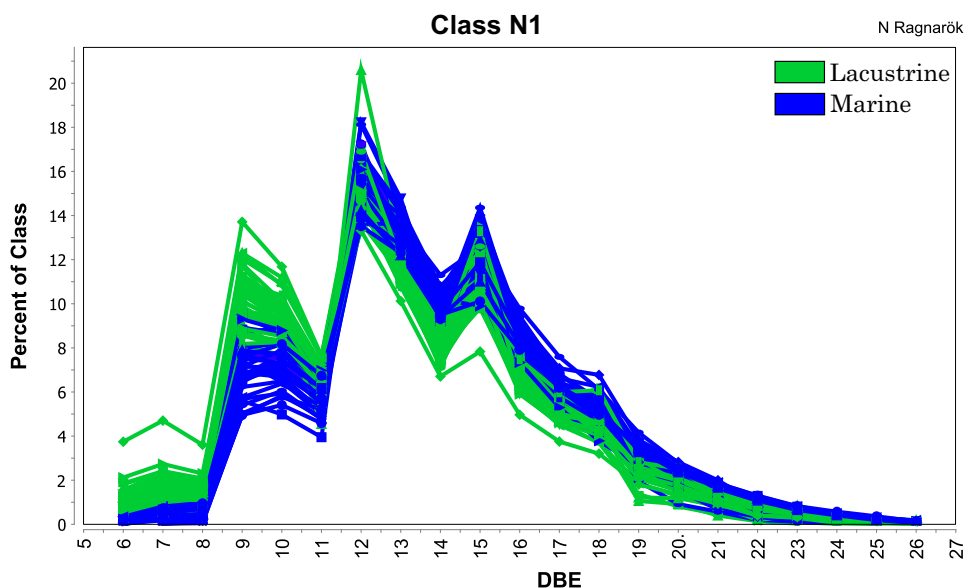
Fig. 7. Distribution of N1-class measured in ESI negative ion mode. Plots show the distributions of these molecular types, sorted into groups of double bond equivalent pseudohomologs (DBE) versus a "Percent of Class" plot (sum of the intensities of all components within one DBE group normalized to the sum of all assigned peak abundances of one (heteroatom) class measured in one ionization mode.

according to differences in their chemical compositions assessed by negative ESI FTICR-MS analysis.

To improve the geochemical characterization by negative ESI FTICR-MS, specifically its potential to differentiate oils generated by different types of source rocks, it is necessary, therefore, to expand the study of polar compounds to include the DBE distribution of the detected classes. The DBE distribution of the four most abundant classes including N1, N1O1, O1, and O2 are described below.

4.3. Detailed characterization of the N1 class

Previous studies showed that the N1 class significantly contributes to oil and bitumen composition. It has been reported that lacustrine oils contain relatively high abundances of N classes and that carbazoles, benzocarbazoles, and dibenzocarbazoles (N1 species with DBEs of 9, 12 and 15, respectively) are present in oils from different sources (Rocha et al. (2018) and references therein).

In the present study, the N1 species are the dominant heteroatomic class found in all crude oil samples analyzed, with DBE values ranging from 6 to 26 (mainly 9–18) regardless of the source rock origin (Fig. 7). Species containing pyrrolic nucleus dominate the DBE distribution of the N1 class and are represented mostly by carbazoles (lacustrine oils: 8.20–13.70% – average: 10.39%; marine oils: 4.90–9.50% – average: 6.97%), benzocarbazoles (lacustrine oils: 13.30–20.60% – average: 15.50%; marine oils: 13.50–18.10% – average: 15.58%) and dibenzocarbazoles (lacustrine

oils: 7.80–13.60% – average: 11.10%; marine oils: 9.90–14.20% – average: 12.19%). A comparison of the distribution of greater DBE values of N1 class from lacustrine and marine oils is shown in Fig. 8. Note that lower DBE values (up to 10) are more abundant in lacustrine than marine oil samples. An equilibrium in these distributions can be observed at DBE 11 and 12. Higher DBE values seem to be more abundant in marine oils, as demonstrated by DBE 13–19.

The statistical analysis has been conducted considering each DBE value with its relative abundance within the class as a different variable. In the HCA plot (Supplementary Fig. 3), two primary domains are present, named as lacustrine and marine. The potential of using the N1 species for geochemical characterization seems to be high, considering that 94% of samples were correctly grouped according to its origin. The same set of data was also analyzed by PCA. Each sample is displayed on a two-dimensional plot (Fig. 9) where the axes correspond to the first two principal components (factors 1 and 2). Factor 1 has a variance of more than 80%, and factor 2 has a variance of 8.4%. Consequently, the total variance of the two components accounts for almost 90% of the variation of the original data. Fig. 9 displays another PCA plot where the DBE values are selected for this analysis and their relationship is explored. Statistical analysis confirmed that marine oils could be related to higher DBE values, whereas lacustrine oils are related to lower DBE values. Essentially, PCA results were considered better than those obtained by HCA analysis because it was possible to individualize two independent domains according to the origin of the sample.
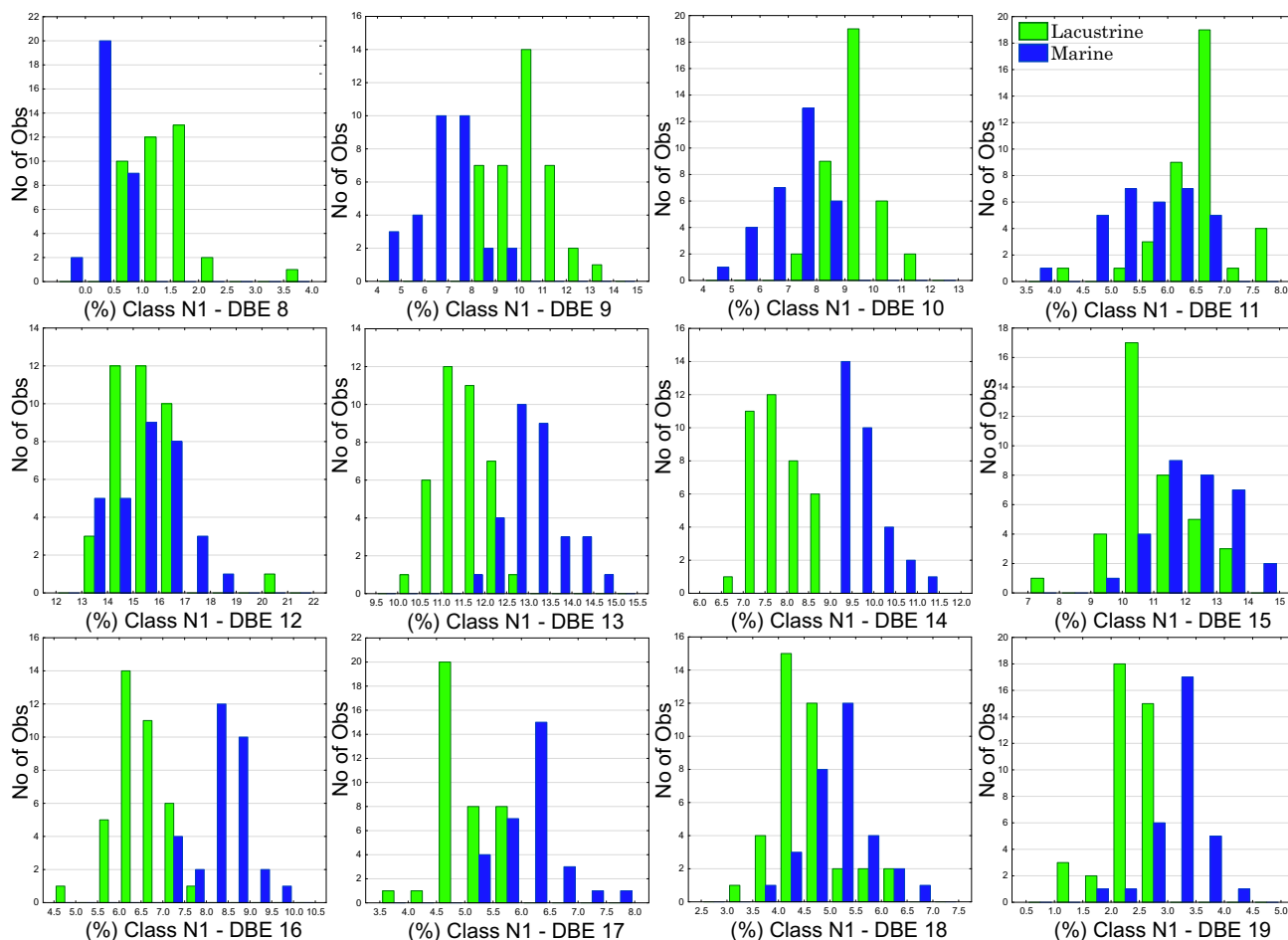
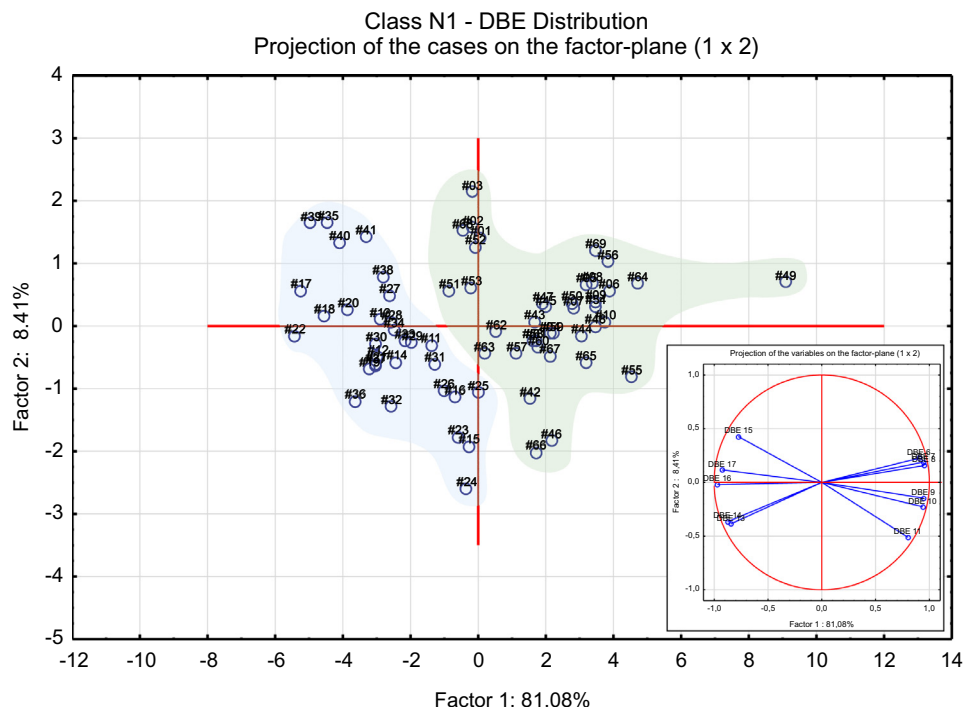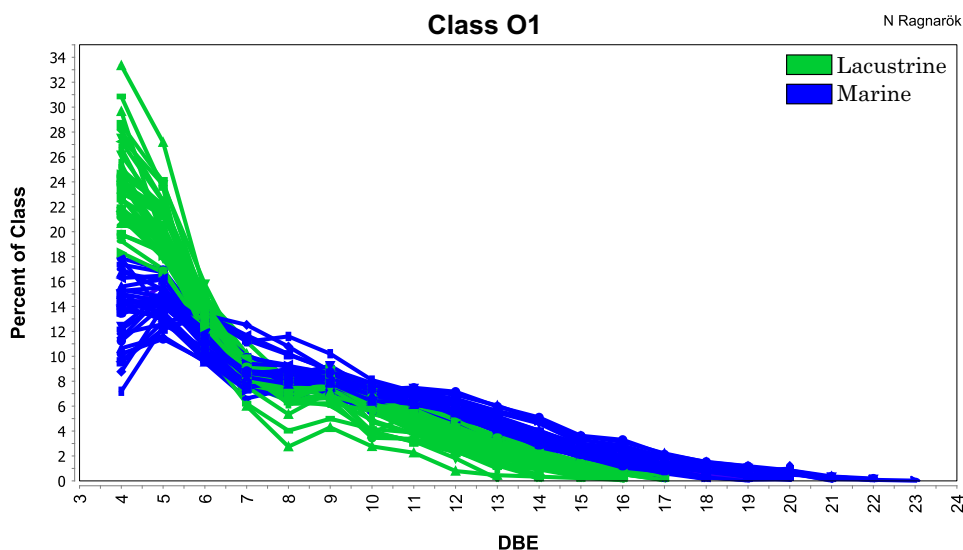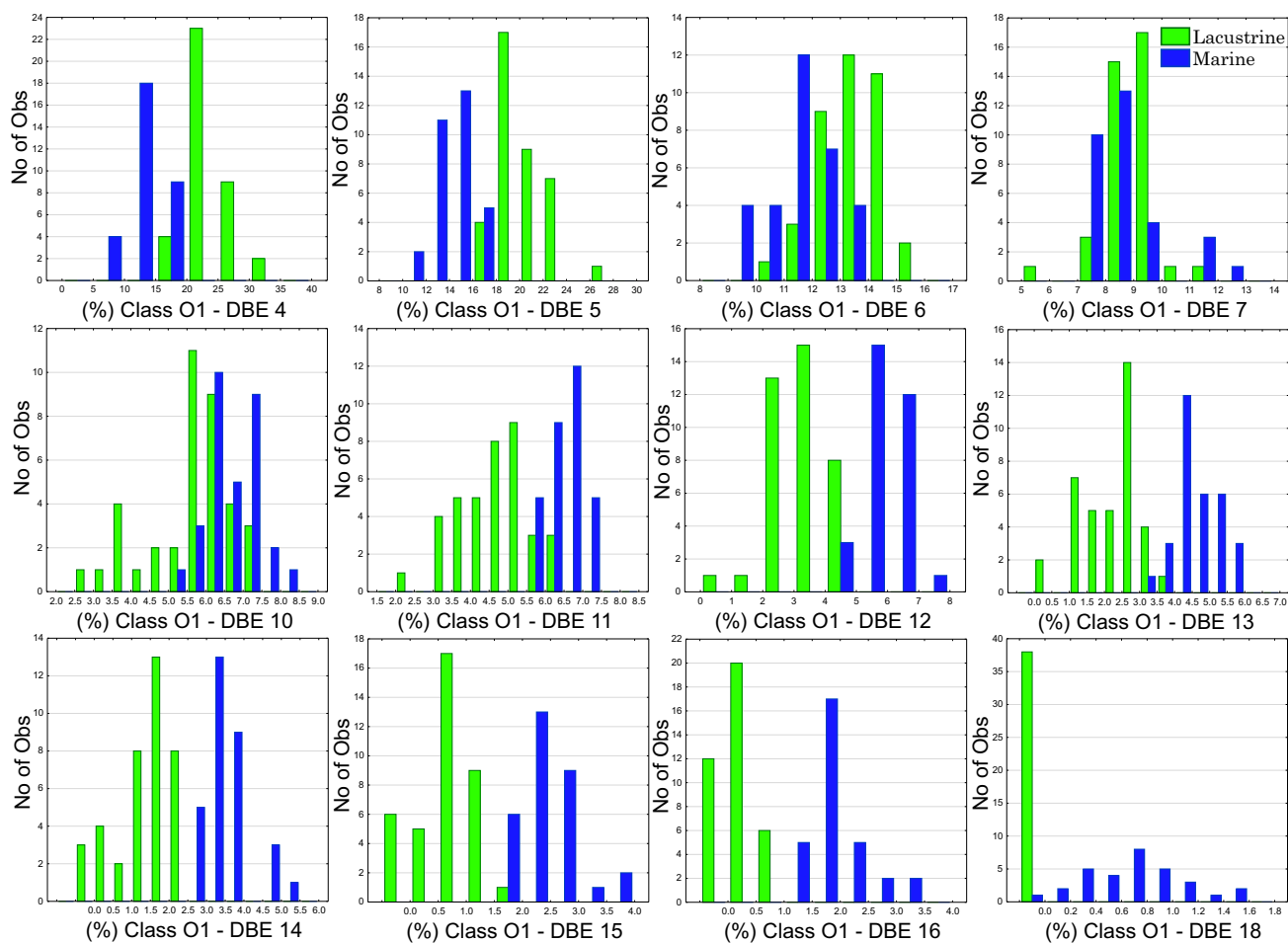**Fig. 8.** Histograms displaying selected DBE groups distribution of the N1-class on the negative ESI FTICR-MS results from the 69 samples analyzed. The samples were split into two domains: marine and lacustrine oil samples.

Thermal evolution processes result in an increase of aromatic species, which means an enrichment of species with high DBE values (Oldenburg et al., 2014; Mahlstedt et al., 2016; Rocha et al., 2018). In these studies, the samples evaluated were generated under a thermal condition related to the peak of oil window. Thus, the enrichment of species with higher DBE values observed for marine oils were attributed to differences in kerogen type. The kerogen type reflects the original biological sources and organic matter content, and with different degrees of aromatization and condensation of their constituents from thermal evolution, the differences between marine and terrestrial kerogens further increase (Vandenbroucke and Largeau, 2007).

According to Mullins et al. (2007), Type I kerogen (originates typically from alginites in lacustrine environments) contains large lipid portions, significant aliphatic groups and low proportions of aromatic units. These authors also reported that Type II kerogen (typically present in marine sediments) contains more aromatic units than Type I kerogen. This statement is in agreement with another study where negative ESI FTICR-MS data of source rock extracts with varied kerogen types showed an increase of the relative abundance of N1 species with high DBE values from Type I kerogen to Type III kerogen (Wan et al., 2017), reflecting increased aromatization and/or condensation in Type II and III kerogens.

Fig. 9. PCA analysis on the DBE groups distribution of the N1-class on the negative ESI FTICR-MS results from the 69 samples analyzed. The projection of the cases and variables are both plotted in the figure.

Fig. 10. Distribution of O1-class measured in ESI negative ion mode. Plots show the distributions of these molecular types, sorted into groups of double bond equivalent pseudohomologs (DBE) versus a "Percent of Class" plot (sum of the intensities of all components within one DBE group normalized to the sum of all assigned peak abundances of one (heteroatom) class measured in one ionization mode.

Fig. 11. Histograms displaying selected DBE groups distribution of the O1-class on the negative ESI FTICR-MS results from the 69 samples analyzed. The samples were split into two domains: marine and lacustrine oil samples.
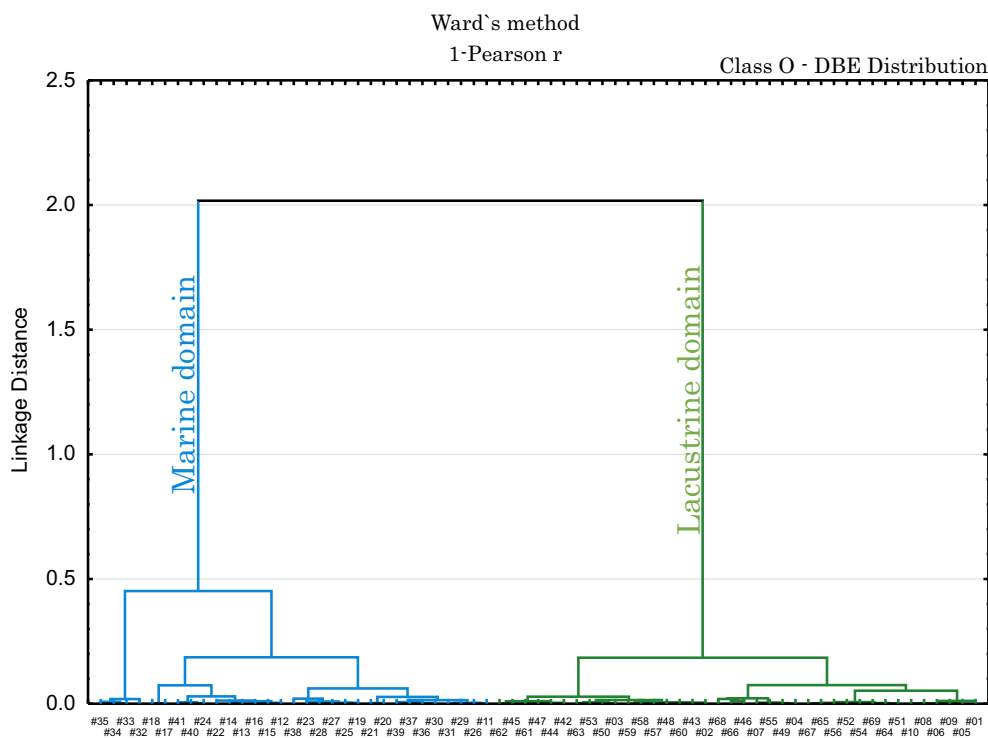
Fig. 12. HCA performed on all O1-class DBE distribution assigned in the negative ESI FTICR-MS results from the 69 samples analyzed.

4.4. Detailed characterization of the O1 class

O1 class species are the second most abundant heteroatom class found either in lacustrine and marine samples and they have a DBE value distribution ranging from 4 to 23 (Fig. 10). The O1 class species are more abundant at a DBE value of 4 (lacustrine oils: 18.30–33.30% – average: 23.90%; marine oils: 7.20–17.90% – average: 13.53%) and a DBE value of 5 (lacustrine oils: 16.70–27.20% – average: 20.24%; marine oils: 11.40–16.90% – average: 14.29%). In addition, the relative abundance of O1 class species decreases gradually as the DBE value increases.

The distributions of major DBE values in lacustrine and marine oils are compared using histograms as shown in Fig. 11. It is found that relative abundances of DBE values of 4 and 5 are higher in lacustrine oils than in marine oil samples. An equilibrium in these distributions can be observed at DBE 6 and 7. In contrast, DBE values ranging from 8 to 17 are relatively enriched in marine oil samples. DBE values higher than 18 were found only in oils derived from source rocks deposited in the marine environment.

The compounds that comprehend O1 class are most likely components with a hydroxyl functional group that is able to be deprotonated (Oldenburg et al., 2014) and related to phenolic compounds (Shi et al., 2010). The occurrence of O1 class is commonly reported in crude oil and source rocks (Pereira et al., 2013; Vaz et al., 2013; Cui et al., 2014; Poetz et al., 2014; Mahlstedt et al., 2016; Oldenburg et al., 2017; Wan et al., 2017).

The results from the statistical analyses considering each DBE distribution from O1 class species reveal a potential method to characterize the origin of crude oil, because both HCA and PCA analysis were able to group the samples 100% correctly according to their origin (Figs. 12 and 13, respectively). Therefore, these results seem to support that oxygenated species might either reflect differences in the originating biomass or indicate a more oxic environment at the time of deposition, as proposed by Hughey et al. (2002).

Regarding the distribution of carbon number related to O1 class, the DBE 4 and DBE 5 pattern distributions stand out. All oil samples analyzed show a normal distribution with a remarkable enrichment at species with 27 and 28 carbon atoms (Fig. 14). Interestingly, O1 class species with DBE values of 4 and 5 could be related to sterols even though their occurrence is not often reported in crude oils (Shi et al., 2010; Oldenburg et al., 2014).

4.5. Detailed characterization of the O2 class

The O2 class species detected by negative ESI FTICR-MS in crude oils is mostly attributed to carboxylic acids, and the O2 class species with DBE 1 are considered as fatty acids (Kim et al., 2005; Li et al., 2010; Vaz et al., 2013; Wan et al., 2017). Lacustrine samples have DBE values ranging from 1 to 17, while marine oils show a more extensive range of DBE values from 1 to 25 (Fig. 15). Overall, there is a strong predominance of DBE 1 in lacustrine oils (20.90–68.20% – average: 30.50%) with the relative abundance gradually decreasing toward higher DBE values. For marine oils there is a significant contribution of fatty acids (6.70–34.70% – average: 18.57%), and a remarkable increase of higher DBE contribution is noted.

Fatty acids in crude oils can be inherited from source rock and directly linked to the kerogen type. Therefore, the higher relative abundance of DBE 1 in lacustrine oils could be associated with Type I kerogen that presents a high initial H/C atomic ratio and a low O/C ratio, with a large amount of lipidic material containing aliphatic chains and a low content in polyaromatic nuclei and heteroatomic bonds.

As DBE 5 and 6 of class O2 represent, respectively, steranoic and hopanoic acids, the carbon number distributions of the oil samples were plotted (Fig. 14). The distribution of carbon numbers ranges from 16 to 54 and 15 to 53 for DBE 5 and 6, respectively. For DBE 5, the relative abundance is higher in the carbon number range of 27 to 32, including cholestanic, ergostanic, and stigmastanic acids
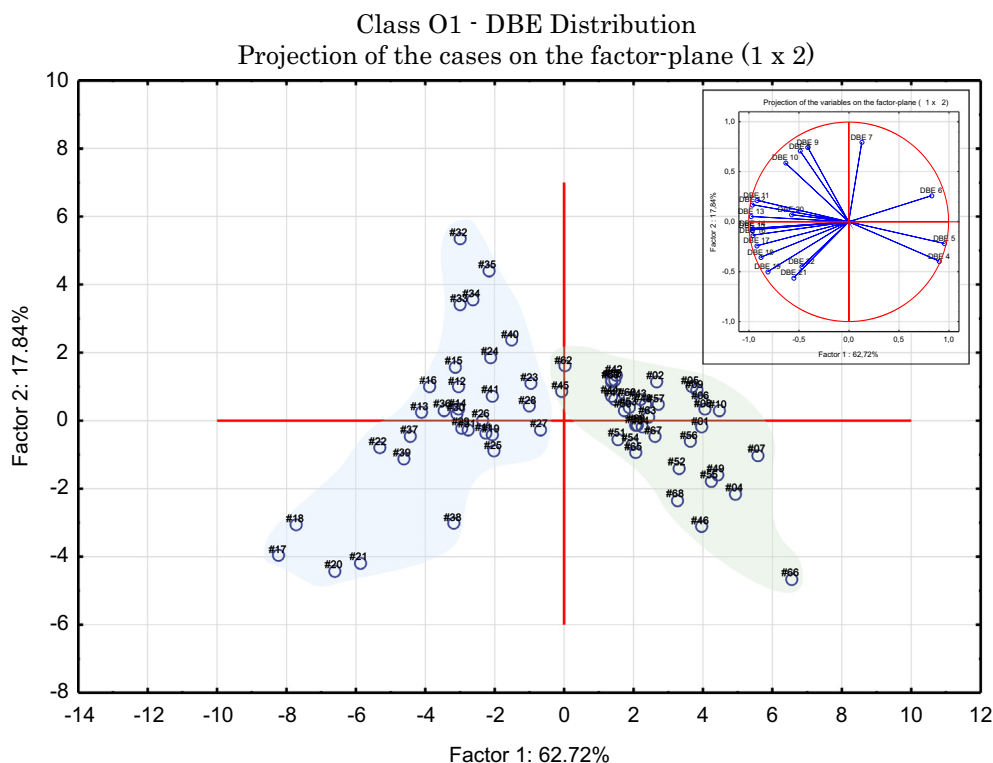

Fig. 13. PCA analysis on the DBE groups distribution of the O1-class on the negative ESI FTICR-MS results from the 69 samples analyzed. The projection of the cases and variables are both plotted in the figure.
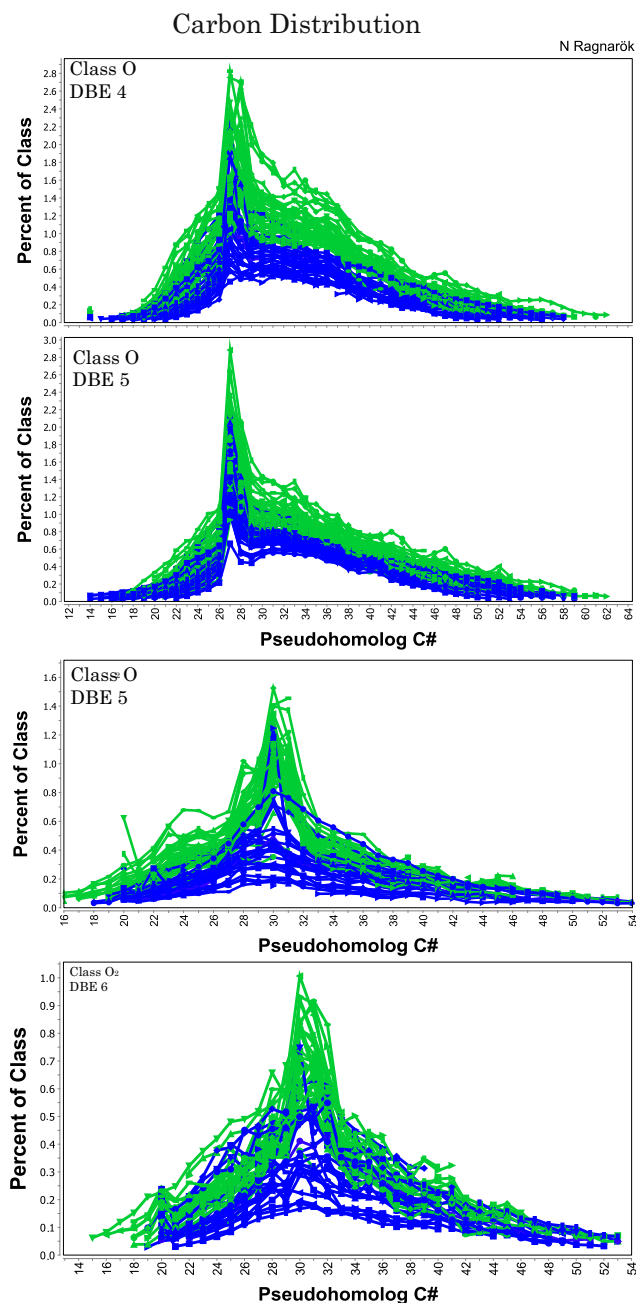
Carbon Distribution

N Ragnarök

Fig. 14. Distribution (from top to bottom) of DBE 4 and 5 compound groups of the O1-class and DBE 5 and 6 compound groups of the O2-class sorted by pseudohomolog carbon number C# versus the fraction of the total heteroatom class measured in ESI negative ion mode.

(O2 class species with DBE 5 and 27, 28, and 29 carbon atoms); DBE 6 ranges mainly from 28 to 34 carbon numbers and could be linked to hopanoic acids (Poetz et al., 2014).

4.6. Detailed characterization of the N1O1 class

The N1O1 class species in the crude oils associated with lacustrine source rocks show DBE values from 5 to 26 (mainly 10–18), and those from marine origin have DBE values from 7 to 26 (mainly 14–21) (Fig. 16). When comparing the two oil groups in Fig. 16, it is noteworthy that type II kerogen produces oils enriched in higher DBE values, related to the increase of aromatic content in kerogen composition.

The distribution of major DBE values of lacustrine oils are compared to that of the marine oil samples using histograms as shown in Fig. 17. It is possible to verify that relative abundances of DBE values ranging from 8 to 13 are higher in lacustrine oils than in marine oil samples. An equilibrium in these distributions can be observed at DBE 14, which is also an inflection point, where DBE values for lacustrine oils start to progressively decrease.

The statistical analysis was designed considering each DBE distribution for N1O1 class species as a different variable. The HCA plot (Supplementary Fig. 4) shows that DBE distribution for the N1O1 class was able to distinguish the two domains labeled lacustrine and marine. The potential of geochemical characterization using the N1O1 species seems to also be high, considering that almost 96% of samples were correctly grouped according to their origin. The set of data was also analyzed by PCA (Fig. 18), and the results were considered better than those obtained with HCA, since it was possible to individualize two independent domains according to the origin of the sample. Factor 1 has a variance of approximately 65% and factor 2 has a variance of 15%. Consequently, the total variance of the two components accounts for almost 80% of the variation of the original data. In Fig. 18, another PCA showing the DBE values used during this analysis and their relationship is plotted, which indicates a strong influence of the use of lower versus higher DBE values on the classification of the samples.

5. Geochemical characterization of polar compounds to assess source discrimination

Several studies have explored the possibility of distinguishing crude oil and source rock origins using petroleomics (Hughey et al., 2002; Wan et al., 2017). Hughey et al. (2002) analyzed three crude oils from North America, Middle East, and China. Wan et al. (2017) analyzed 22 crude oils and 19 source rock samples from Nanpu Sag. In both publications, the authors agreed that the concentration and the distribution of heteroatomic compounds vary according to geological origins of oils and their related source rocks. Chiaberge et al. (2013) examined a set of 14 samples and demonstrated how molecular characterization of crude oils with APPI- FTICR-MS, in combination with statistical analysis such as PCA and HCA, can provide significant information regarding the geographical location and the well from which oil has been extracted. In the present work, sixty-nine crude oil samples were analyzed from 4 different Brazilian offshore basins, and the results demonstrated that detailed characterization of N1, O1, O2 and N1O1 species present in crude oils from the lacustrine and marine origin by negative-ion ESI FTICR-MS could be used to identify the geochemical origin of crude oils. In summary, we have plotted ternary diagrams (Supplementary Fig. 5) to demonstrate the potential of a quick data treatment for an efficient source discrimination. Additionally, the relationship between the sum of the relative abundance of these four classes with low DBE values high DBE values [Class N $\sum$DBE 6–10/($\sum$DBE 6–10/$\sum$DBE 10–27); Class NO $\sum$DBE 2–14/($\sum$DBE 2–14/$\sum$DBE15-29); Class O $\sum$DBE 4–10/($\sum$DBE 4–10/$\sum$DBE 11–23); Class O2 $\sum$DBE 1–7/($\sum$DBE 1–7/$\sum$DBE 8–25)] was examined in order to perform oil-oil correlation to differentiate the four studied basins according to the origin of the samples – marine and lacustrine (Fig. 19a and b). To refine the characterization of those crude oil samples, specific DBE values from the major classes were selected considering the histograms distributions of each class and other two ratios was created [(Class N $\sum$DBE 8–9) + (Class NO $\sum$DBE 9–10)/(Class N $\sum$DBE 8,9,13,16) + (Class NO $\sum$DBE 9,10,19,20); (Class O $\sum$DBE 4,12) + (Class O2 DBE 12)/(Class O $\sum$DBE 4,12,14,16) + (Class O2 $\sum$DBE 12,13)] (Fig. 19c). Tentatively, a plot of Class NO DBE 10 and Class O DBE 4 was
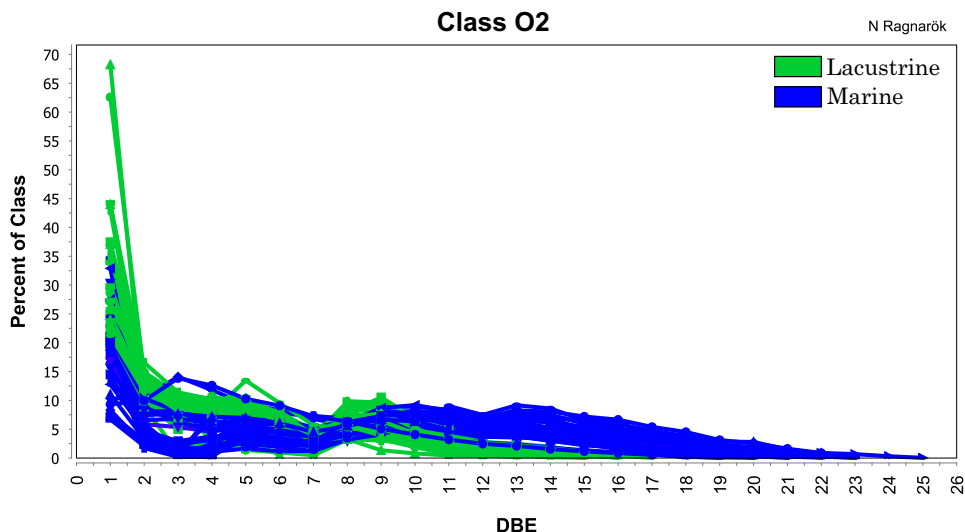
Fig. 15. Distribution of O2-class measured in ESI negative ion mode. Plots show the distributions of these molecular types, sorted into groups of double bond equivalent pseudohomologs (DBE) versus a "Percent of Class" plot (sum of the intensities of all components within one DBE group normalized to the sum of all assigned peak abundances of one (heteroatom) class measured in one ionization mode.
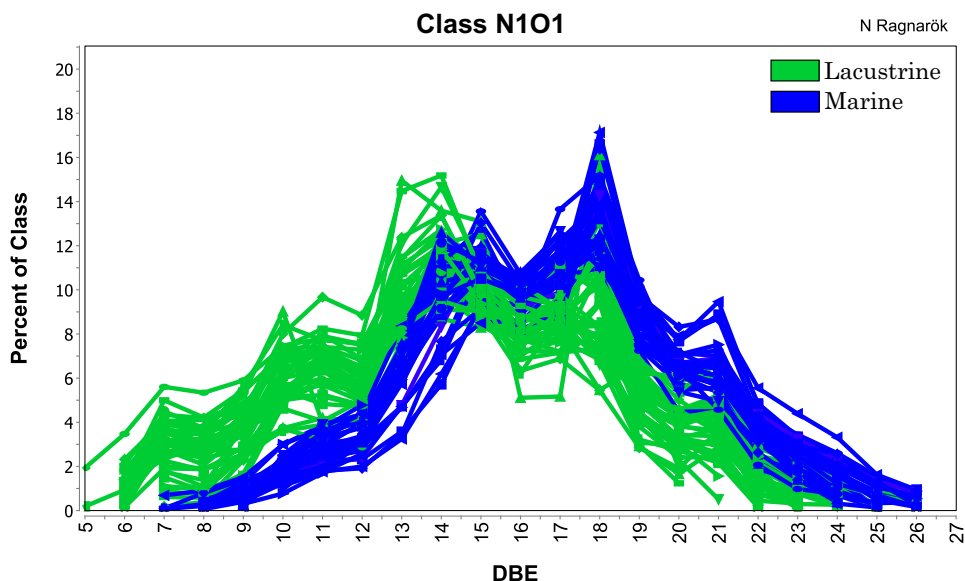

Fig. 16. Distribution of N1O1-class measured in ESI negative ion mode. Plots show the distributions of these molecular types, sorted into groups of double bond equivalent pseudohomologs (DBE) versus a "Percent of Class" plot (sum of the intensities of all components within one DBE group normalized to the sum of all assigned peak abundances of one (heteroatom) class measured in one ionization mode.

created for a quick oil-oil correlation (Fig. 19d). In general, an excellent relationship between the oils and their origin was obtained, validating that negative ESI FTICR-MS can be used as a tool for geochemical assessment of crude oils.

6. Conclusions

Several species from many different classes were directly detected in the sixty-nine crude oil samples by negative ESI FTICR-MS analyses. The FTICR-MS technique enables a molecular-level analysis of complex mixtures with accurate mass measurements and provides information on unique elemental compositions.

Lacustrine oils tend to be enriched in Nx compounds, while marine oils can be distinguished by dominance of Ox compounds.

The dominant class species in the studied crude oils is N1, followed by O1, O2, and N1O1 with remarkable differences between marine and lacustrine distribution.

Kerogen type plays an important role in the heteroatomic profile of the crude oils analyzed. Organic matter from kerogen Type I has high H/C atomic ratio and low oxygen content, while organic matter from Type II kerogen contains higher O/C atomic ratio and high abundance of carboxylic acid groups and ester groups. Such differences result in a clear separation based on polar species found in marine and lacustrine oils generated from Type I and Type II kerogens.

Oil-oil correlations show that large differences exist in the DBE distribution of four selected heteroatomic classes of crude oils, allowing a quick geochemical assessment regarding their origin. These characteristics enabled us to create four ratios that describe the relationship between the sum of the relative abundances of
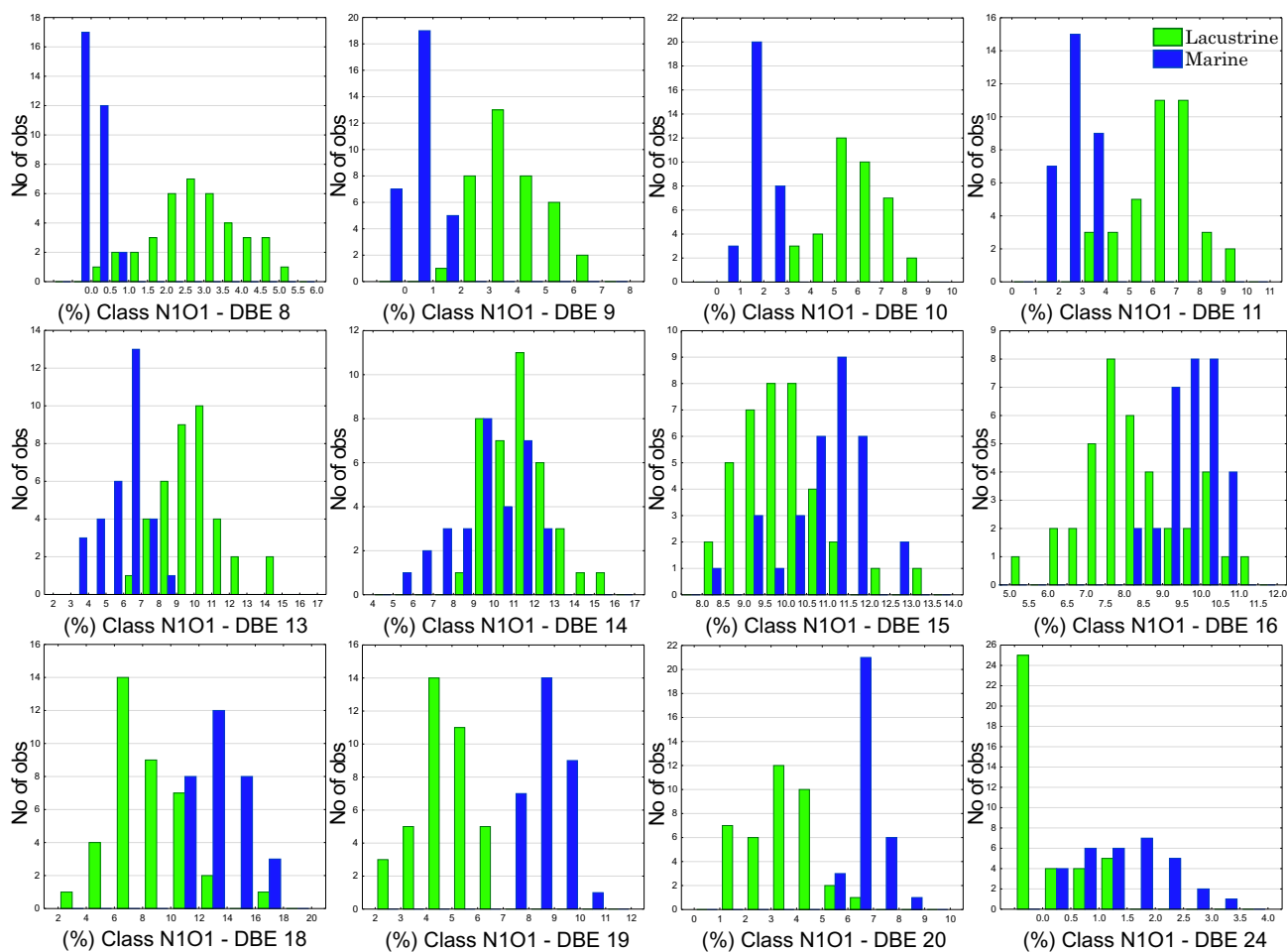
Fig. 17. Histograms displaying selected DBE groups distribution of the N1O1-class on the negative ESI FTICR-MS results from the 69 samples analyzed. The samples were split into two domains: marine and lacustrine oil samples.
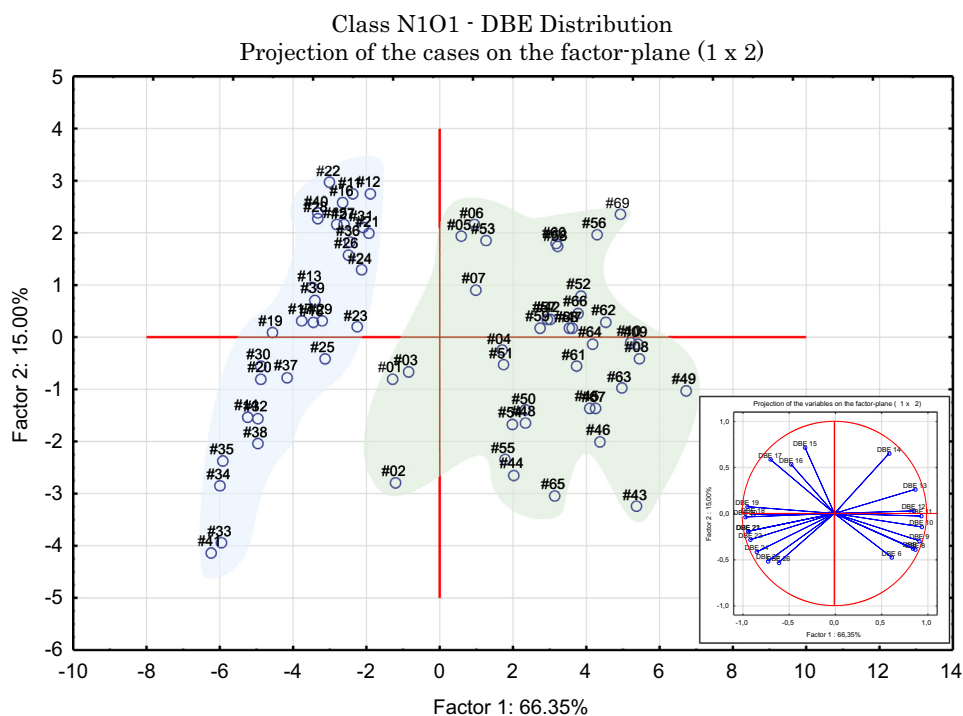

Fig. 18. PCA analysis on the DBE groups distribution of the N1O1-class on the negative ESI FTICR-MS results from the 69 samples analyzed. The projection of the cases and variables are both plotted in the figure.
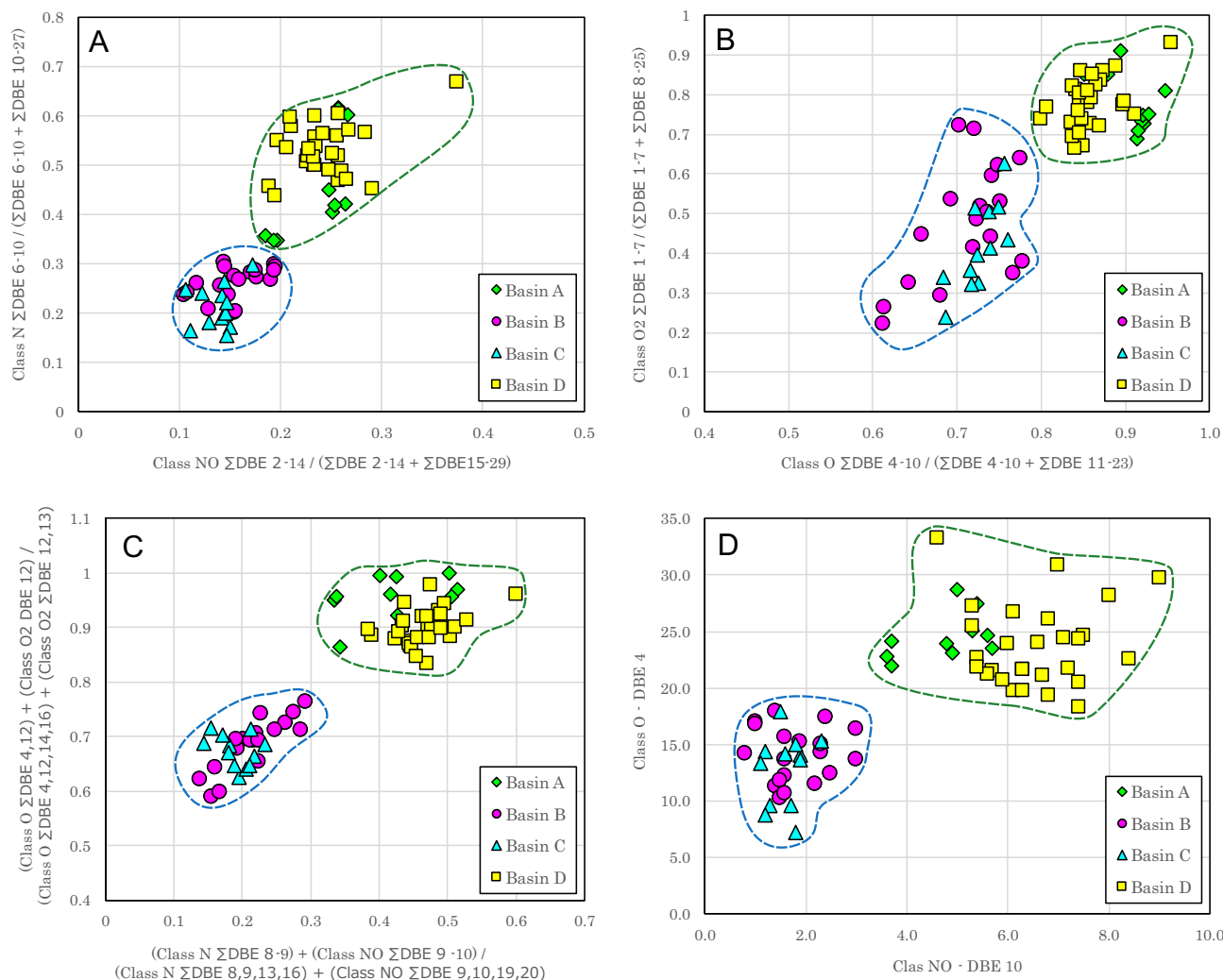
Fig. 19. Oil-oil correlations and geochemical assessment by cross-plots of exclusive parameters from negative ESI FTICR-MS results.

these four classes and low DBE values versus high DBE values [Class N1 $\sum$DBE 6–10/($\sum$DBE 6–10 + $\sum$DBE 10–27); Class N1O1 $\sum$DBE 2–14/($\sum$DBE 2–14 + $\sum$DBE 15–29); Class O1 $\sum$DBE 4–10/ ($\sum$DBE 4–10 + $\sum$DBE 11–23); Class O2 $\sum$DBE 1–7/($\sum$DBE 1–7 + $\sum$DBE 8–25)]. Furthermore, selected DBE values from N1, N1O1, O1, and O2 were chosen to refine the characterization of the lacustrine and marine oils. For a quick oil-oil correlation, Class NO DBE 10 and Class O DBE 4 plot is recommended for Brazilian off-shore crude oils.

The use of negative ESI FTICR-MS as a geochemistry tool and its combination with multivariate statistical analysis can add information to the current methods used for geochemical assessment, allowing the full comprehension of crude oil composition.

Appendix A. Supplementary material

Supplementary data associated with this article can be found, in the online version, at https://doi.org/10.1016/j.orggeochem.2018. 05.012.

Associate Editor—**Clifford C. Walters**

References

Casilli, A., Silva, R.C., Laakia, J., Oliveira, C.J.F., Ferreira, A.A., Loureiro, M.R.B., Azevedo, D.A., Aquino Neto, F.R., 2014. High resolution molecular organic geochemistry assessment of Brazilian lacustrine crude oils. Organic Geochemistry 68, 61–70.

Chiaberge, S., Fiorani, T., Savoini, A., Bionda, A., Ramello, S., Pastori, M., Cesti, P., 2013. Classification of crude oil samples through statistical analysis of APPI FTICR mass spectra. Fuel Processing Technology 106, 181–185.

Contreras, J., Zühlke, R., Bowman, S., Bechstädt, T., 2010. Seismic stratigraphy and subsidence analysis of the southern Brazilian margin (Campos, Santos and Pelotas basins). Marine and Petroleum Geology 27, 1952–1980.

Cui, J., Zhu, R., Hu, J., 2014. Identification and geochemical significance of polarized macromolecular compounds in lacustrine and marine oils. Chinese Journal of Geochemistry 33, 431–438.

Dembicki, H., 2016. Practical Petroleum Geochemistry for Exploration and Production. Elsevier, p. 342.

Hughey, C.A., Galasso, S.A., Zumberge, J.E., 2007. Detailed compositional comparison of acidic NSO compounds in biodegraded reservoir and surface crude oils by negative ion electrospray Fourier transform ion cyclotron resonance mass spectrometry. Fuel 86, 758–768.

Hughey, C.A., Rodgers, R.P., Marshall, A.G., Qian, K., Robbins, W.K., 2002. Identification of acidic NSO compounds in crude oils of different gochemical origins by negative-ion electrospray Fourier transform ion cyclotron resonance mass spectrometry. Organic Geochemistry 33, 743–759.

Katz, B.J., Mello, M.R., 2000. Petroleum systems of south atlantic marginal basins – an overview. American Association of Petroleum Geologists Memoirs 73, 1–13.

Kim, S., Stanford, L.A., Rodgers, R.P., Marshall, A.G., Walters, C.C., Qian, K., Wenger, L.M., Mankiewicz, P., 2005. Microbial alteration of the acidic and neutral polar NSO compounds revealed by Fourier transform ion cyclotron resonance mass spectrometry. Organic Geochemistry 36, 1117–1134.

Krawczyk, W., Kunda, T., Perkowska, I., Dudek, D., 2005. Impurity profiling/comparative analyses of samples of 1-phenyl-2-propanone. Bulletin on Narcotics, Volume LVII, Nos. 1 and 2. United Nation Office on Drugs and Crime.

Laakia, J., Casilli, A., Araújo, B.Q., Gonçalves, F.T.T., Marotta, E., Oliveira, C.J.F., Carbonezi, C.A., Loureiro, M.R.B., Azevedo, D.A., Aquino Neto, F.R., 2017. Characterization of unusual tetracyclic compounds and possible novel maturity parameters for Brazilian crude oils using comprehensive two-dimensional gas chromatography-time of flight mass spectrometry. Organic Geochemistry 106, 93–104.

Li, M., Cheng, D., Pan, X., Dou, L., Hou, D., Shi, Q., Wen, Z., Tang, Y., Achal, S., Milovic, M., Tremblay, L., 2010. Characterization of petroleum acids using combined FT-IR, FT-ICR-MS and GC-MS: implications for the origin of high acidity oils in the Muglad Basin, Sudan. Organic Geochemistry 41, 959–965.

Liu, P., Li, M., Jiang, Q., Cao, T., Sun, Y., 2015. Effect of secondary oil migration distance on composition of acidic NSO compounds in crude oils determined by negative-ion electrospray Fourier transform ion cyclotron resonance mass spectrometry. Organic Geochemistry 78, 23–31.

Mahlstedt, N., Horsfield, B., Wilkes, H., Poetz, S., 2016. Tracing the impact of fluid retention on bulk petroleum properties using nitrogen-containing compounds. Energy & Fuels 30, 6290–6305.

Marshall, A.G., Hendrickson, C.L., Emmett, M.R., Rodgers, R.P., Blakney, G.T., Nilsson, C.L., 2007. Fourier transform ion cyclotron resonance: state of the art. European Journal of Mass Spectrometry 13, 57–59.

Mello, M.R., De Azambuja Filho, N.C., Bender, A.A., Barbanti, S.M., Mohriak, W., Schmitt, P., de Jesus, C.L.C., 2012. The Namibian and Brazilian southern South Atlantic petroleum systems: are they comparable analogues? Geological Society, London, Special Publications, 249–266.

Mello, M.R., Gaglianone, P.C., Brassell, S.C., Maxwell, J.R., 1988. Geochemical and biological marker assessment of depositional environments using Brazilian offshore oils. Marine and Petroleum Geology 5, 205–223.

Mello, M.R., Koutsoukos, E.A.M., Santos Neto, E. V., da Silva-Telles Jr., A.C., 1993. Geochemical and Micropaleontological Characterization of Lacustrine and Marine Hypersaline Environments from Brazilian Sedimentary Basins. In: Katz, J.B., Pratt, L.M. (Eds.), Source Rock in a Sequence Stratigraphic Framework. American Association of Petroleum Geologists Memoirs Studies in Geology, vol. 37, pp. 17–34.

Mello, M.R., Telnaes, N., Maxwell, J.R., 1995. The hydrocarbon source potential in the Brazilian marginal basins: a geochemical and paleo- environmental assessment. Paleogeography, Paleoclimate, and Source Rock 40, 233–272.

Miller, J.N., Miller, J.C., 2010. Statistics and chemometrics for analytical chemistry. Pearson Education, Canada.

Mullins, O.C., Sheu, E.Y., Hammami, A., Marshall, A.G., 2007. Asphaltenes, heavy oils, and petroleomics. Springer, New York.

Oldenburg, T.B.P., Brown, M., Bennett, B., Larter, S.R., 2014. The impact of thermal maturity level on the composition of crude oils, assessed using ultra-high resolution mass spectrometry. Organic Geochemistry 75, 151–168.

Oldenburg, T.B.P., Jones, M., Huang, H., Bennett, B., Shafiee, N.S., Head, I., Larter, S.R., 2017. The controls on the composition of biodegraded oils in the deep subsurface- Part 4. Destruction and production of high molecular weight non-hydrocarbon species and destruction of aromatic hydrocarbons during progressive in-reservoir biodegradation. Organic Geochemistry 114, 57–80.

Pereira, R.C.L., Simas, R.C., Corilo, Y.E., Vaz, B.G., Klitzke, C.F., Schmidt, E.M., Pudenzi, M.A., Silva, R.M.C.F., Moraes, E.T., Bastos, W.L., Eberlin, M.N., Nascimento, H.D.L., 2013. Precision in petroleomics via ultrahigh resolution electrospray ionization fourier transform ion cyclotron resonance mass spectrometry. Energy & Fuels 27, 7208–7216.

Peters, K.E., Walters, C.C., Moldowan, J.M., 2005. The Biomarker Guide. Cambridge University Press, Cambridge.

Poetz, S., Horsfield, B., Wilkes, H., 2014. Maturity-driven generation and transformation of acidic compounds in the organic-rich posidonia shale as revealed by electrospray ionization fourier transform ion cyclotron resonance mass spectrometry. Energy & Fuels 28, 4877–4888.

Qian, K., Rodgers, R.P., Hendrickson, C.L., Emmett, M.R., Marshall, A.G., 2001. Reading chemical fine print: Resolution and identification of 3000 nitrogen-containing aromatic compounds from a single electrospray ionization Fourier transform ion cyclotron resonance mass spectrum of heavy petroleum crude oil. Energy and Fuels 15, 492–498.

Rocha, Y.S., Pereira, R.C.L., Mendonça Filho, J.G., 2018. Negative electrospray Fourier transform ion cyclotron resonance mass spectrometry determination of the effects on the distribution of acids and nitrogen-containing compounds in the simulated thermal evolution of a Type-I source rock. Organic Geochemistry 115, 32–45.

Rodgers, R.P., Schaub, T.M., Marshall, A.G., 2005. PETROLEOMICS: MS Returns to Its Roots. Analytical Chemistry 77, 20 A-27 A.

Schiefelbein, C.F., Zumberge, J.E., Cameron, N.C., Brown, S.W., 2000. Geochemical comparison of crude oil along the South Atlantic margins. American Association of Petroleum Geologists Memoir 73, 15–26.

Schiefelbein, C.F., Zumberge, J.E., Cameron, N.R., Brown, S.W., 1999. Petroleum systems in the South Atlantic margins. In: Cameron, N.R., Bate, R.H., Clure, V.S. (Eds.), The Oil and Gas Habitats of the South Atlantic. Geological Society of London, Special Publications, pp. 169–179.

Shi, Q., Zhao, S., Xu, Z., Chung, K.H., Zhang, Y., Xu, C., 2010. Distribution of acids and neutral nitrogen compounds in a Chinese crude oil and its fractions: characterized by negative-ion electrospray ionization Fourier transform ion cyclotron resonance mass spectrometry. Energy and Fuels 24, 4005–4011.

Strozyk, F., Back, S., Kukla, P.A., 2017. Comparison of the rift and post-rift architecture of conjugated salt and salt-free basins offshore Brazil and Angola/Namibia, South Atlantic. Tectonophysics 716, 204–224.

Tissot, B.P., Welte, D.H., 1984. Petroleum Formation and Occurrence. Berlin, Springer-Verlag.

Tong, J., Liu, J., Han, X., Wang, S., Jiang, X., 2013. Characterization of nitrogen-containing species in Huadian shale oil by electrospray ionization Fourier transform ion cyclotron resonance mass spectrometry. Fuel 104, 365–371.

Vandenbroucke, M., Largeau, C., 2007. Kerogen origin, evolution and structure. Organic Geochemistry 38, 719–833.

Vaz, B.G., Silva, R.C., Klitzke, C.F., Simas, R.C., Lopes Nascimento, H.D., Pereira, R.C.L., Garcia, D.F., Eberlin, M.N., Azevedo, D.A., 2013. Assessing biodegradation in the llanos orientales crude oils by electrospray ionization ultrahigh resolution and accuracy fourier transform mass spectrometry and chemometric analysis. Energy and Fuels 27, 1277–1284.

Wan, Z., Li, S., Pang, X., Dong, Y., Wang, Z., Chen, X., Meng, X., Shi, Q., 2017. Characteristics and geochemical significance of heteroatom compounds in terrestrial oils by negative-ion electrospray Fourier transform ion cyclotron resonance mass spectrometry. Organic Geochemistry 111, 34–55.